

# An Exact Sampler for Inference after Polyhedral Model Selection

Sifan Liu\*

Department of Statistics, Stanford University

August 2023

## Abstract

Inference after model selection presents computational challenges when dealing with intractable conditional distributions. Markov chain Monte Carlo (MCMC) is a common method for sampling from these distributions, but its slow convergence often limits its practicality. In this work, we introduce a method tailored for selective inference in cases where the selection event can be characterized by a polyhedron. The method transforms the variables constrained by a polyhedron into variables within a unit cube, allowing for efficient sampling using conventional numerical integration techniques. Compared to MCMC, the proposed sampling method is highly accurate and equipped with an error estimate. Additionally, we introduce an approach to use a single batch of samples for hypothesis testing and confidence interval construction across multiple parameters, reducing the need for repetitive sampling. Furthermore, our method facilitates fast and precise computation of the maximum likelihood estimator based on the selection-adjusted likelihood, enhancing the reliability of MLE-based inference. Numerical results demonstrate the superior performance of the proposed method compared to alternative approaches for selective inference.

## 1 Introduction

Inference after model selection must account for selection bias. One approach to correct the selection bias is to condition on the event of model selection. Through this conditioning, information utilized for selection is discarded, leaving only residual information for inference. In particular, inference is conducted based on the distribution of the data conditional on the selection event.

A preeminent model selection technique in regression is the lasso (Tibshirani, 1996). This method entails minimizing the negative log-likelihood augmented by an  $\ell_1$  penalty. The introduction of the  $\ell_1$  penalty favors a parsimonious estimator of the regression coefficients, leading to convenient variable selection. The distribution of the least-squares estimator of a coefficient within the selected model, after conditioning on the selection event as well as the signs of the selected variables and nuisance parameters, is a truncated univariate Gaussian distribution (Lee et al., 2016). Therefore, exact post-selection inference is possible in this case.

---

\*The author thanks Prof. Art Owen, Snigdha Panigrahi, and Jonathan Taylor for helpful conversations. This work was partially funded by the NSF grant DMS-2152780 and the Stanford Data Science Scholars program. Correspondence email: [sfliu@stanford.edu](mailto:sfliu@stanford.edu)

However, this approach tends to yield excessively long confidence intervals due to the over-conditioning, which leaves little information for inference. In fact, it has been shown that this type of confidence interval has infinite expected length (Kivaranovic and Leeb, 2021). To address this issue, randomized versions of the lasso have been proposed to boost the inferential power. For example, Tian et al. (2018) propose to add noise to the response vector and run the lasso on the noisy response. Another approach, known as data carving (Fithian et al., 2014), uses a subset of data for model selection. The two approaches can be shown to be asymptotically equivalent under certain conditions and we refer to both as the randomized lasso. In this situation, the randomness in the selection stage effectively smooths the boundary of the selection event. Consequently, the resulting conditional distribution is no longer a hard-truncated normal distribution, but can be viewed as a soft-truncated normal due to the marginalization over the randomness involved in selection. To conduct inference based on this distribution, prior works often resort to Markov chain Monte Carlo (MCMC) sampling, which is computationally intensive and might suffer from slow mixing, potentially resulting in unreliable inference.

A notable observation is that the lasso, along with several other model selection algorithms, gives rise to selection events that can be delineated as polyhedra when properly conditioned. Such methods, encompassing the lasso (Lee et al., 2016), elastic net (Zou and Hastie, 2005), square-root lasso (Belloni et al., 2011; Tian et al., 2018), forward stepwise regression, least angle regression (Tibshirani et al., 2016), SLOPE (Bogdan et al., 2015), and the Benjamini-Hochberg procedure (Benjamini and Hochberg, 1995; Reid et al., 2017), fall under the category of polyhedral model selection. When the selection event is characterized by a polyhedron, it opens the door to utilizing more specialized sampling techniques tailored to this structure, surpassing the capabilities of generic MCMC algorithms.

Thus, our first contribution is to introduce a more efficient sampling method designed specifically for conducting inference after polyhedral model selection. The method relies on the classic separation-of-variable method (SOV (Genz, 1992)), which transforms the variables constrained by a polyhedron into variables within a unit cube. Subsequently, sampling from the unit cube can be executed with enhanced efficiency by leveraging conventional numerical integration methods, such as randomized quasi-Monte Carlo (QMC). The obtained p-values are highly accurate and equipped with error estimates. Furthermore, we develop a method that uses a single batch of QMC samples to construct confidence intervals for all selected variables, substantially reducing the computational workload.

Some recently proposed inference methods for the randomized lasso bypass the need for sampling. For instance, Panigrahi and Taylor (2022) present the method of approximate selective maximum likelihood estimator (MLE), which is based on the approximate normality of the MLE of the selection-adjusted likelihood. Their method computes the approximate MLE and uses the corresponding Fisher information matrix to construct Wald-type confidence intervals. Although it offers computational efficiency, this approach approximates both the MLE and its corresponding Fisher information matrix, relying on a Laplace approximation of the selection event probability. Consequently, this method is not reliable when the Laplace approximation falters.

To address this issue, our second contribution is an optimization algorithm that directly maximizes the selective likelihood without using any large-deviation type approximations. Our approach involves computing the gradient of the log-likelihood via the SOV technique and subsequently employing gradient ascent. Upon convergence, the SOV method is applied again to evaluate the Hessian at the maximum. Because the SOV method is highly accurate in estimating the gradients and Hessian, this provides a more dependable approach for conducting MLE-based inference after

selection.

The remainder of the paper is structured as follows. In Section 2, we introduce the background of the randomized lasso, and the two approaches for inference: one based on the cumulative distribution function (CDF) of the conditional distribution and one based on selective MLE. We discuss some related work at the end. In Section 3, we introduce the SOV method, which is employed to compute the p-value under the selection-adjusted distribution. Additionally, we propose several variance reduction techniques and present an algorithm designed to construct confidence intervals for all target parameters employing a single set of samples. In Section 4, we elaborate on the utilization of the proposed method for optimizing the selective likelihood and conducting MLE-based inference. To demonstrate the effectiveness of the proposed method, we present numerical results in Section 5. Section 6 has our conclusions. Proofs and additional numerical results are in the Appendix. Code for the algorithm is accessible through the GitHub repository at [https://github.com/liusf15/selinf\\_sampler](https://github.com/liusf15/selinf_sampler).

## 2 Inference after randomized lasso

As mentioned earlier, incorporating randomness during the selection stage preserves more information for subsequent inference, thereby increasing the inferential power. In this section, we delve into the randomized lasso problem and outline the framework for conducting conditional post-selection inference within this context.

### 2.1 Randomized lasso and inference target

Consider a dataset comprising  $n$  data points  $(\mathbf{x}_i, y_i) \in \mathbb{R}^p \times \mathbb{R}$ , where  $y_i$  is the response and  $\mathbf{x}_i$  represents the potentially high-dimensional feature. These observations are organized into the response vector  $Y$  of size  $n$  and the design matrix  $X$  of size  $n \times p$ . We assume a normal homoscedastic model  $Y \sim \mathcal{N}(\boldsymbol{\mu}, \sigma^2 I)$  while leaving  $\boldsymbol{\mu} \in \mathbb{R}^n$  unspecified. We assume  $\sigma^2$  is known in this section.

In scenarios where not all  $p$  features contribute meaningfully to predicting or interpreting the response, a model selection algorithm can be employed to identify a pertinent subset of features. For instance, the lasso (Tibshirani, 1996) solves a regularized optimization problem with the sparsity-inducing  $\ell_1$  penalty. To incorporate randomness into the selection process, we solve the following randomized lasso problem

$$\hat{\boldsymbol{\beta}}^\lambda = \operatorname{argmin}_{\boldsymbol{\beta} \in \mathbb{R}^p} \frac{1}{2} \|Y - X\boldsymbol{\beta}\|_2^2 + \lambda \|\boldsymbol{\beta}\|_1 - \boldsymbol{\omega}^\top \boldsymbol{\beta}, \quad (1)$$

where  $\boldsymbol{\omega} \sim \mathcal{N}_p(\mathbf{0}, \Omega)$  is the randomization variable that is generated independently of the data, and  $\lambda$  stands for the regularization parameter. This formulation can be shown to be asymptotically equivalent to the data carving, which uses a subset of the data for the lasso. Let  $M = \{j \in [p] : \hat{\beta}_j^\lambda \neq 0\}$  denote the set of selected variables and let  $d = |M|$  be the number of selected variables. We will assume the selected model has full rank such that  $\operatorname{rank}(X_M) = d$ .

The inference target within the selected model is often nonstandard. For instance, in the submodel view (Berk et al., 2013), the inference target is defined to be  $X_M^\dagger \mathbb{E}[Y]$ , which is the projection of  $\boldsymbol{\mu} = \mathbb{E}[Y]$  onto the column space spanned by the selected features  $X_M$ . Alternatively, the full model view chooses the inference target to be  $\boldsymbol{\beta}^f := X^\dagger \mathbb{E}[Y]$ , which is well-defined only when  $\operatorname{rank}(X) = p$ . Particularly, the parameters of interest are those  $\beta_j^f$  for  $j \in M$ .

In either case, the inference target can be represented as  $\beta_M = \mathcal{A}_M \mathbb{E}[Y]$  for some  $d \times p$  matrix  $\mathcal{A}_M$  depending on  $M$ . Inference can then be based on

$$\mathcal{A}_M Y \sim \mathcal{N}(\beta_M, \sigma^2 \mathcal{A}_M \mathcal{A}_M^\top). \quad (2)$$

In the submodel view,  $\mathcal{A}_M = X_M^\dagger$ , resulting in  $\mathcal{A}_M Y \sim \mathcal{N}(\beta_M, \sigma^2 (X_M^\top X_M)^{-1})$ , where  $\mathcal{A}_M Y$  coincides with the least-squares estimator by regressing  $Y$  onto the selected variables  $X_M$ . In the full model view,  $\mathcal{A}_M = J_M X^\dagger$ , where  $J_M \in \mathbb{R}^{d \times p}$  consists of the rows of the identity matrix  $I_p$  with indices in  $M$ .

Hereafter, we denote the test statistic as  $\hat{\beta}_M = \mathcal{A}_M Y$  and the covariance matrix as  $\Sigma = \sigma^2 \mathcal{A}_M \mathcal{A}_M^\top$ . Thus, Equation (2), along with  $\omega \sim \mathcal{N}_p(\mathbf{0}, \Omega)$ , leads to

$$\begin{pmatrix} \hat{\beta}_M \\ \omega \end{pmatrix} \sim \mathcal{N}_{d+p} \left( \begin{pmatrix} \beta_M \\ \mathbf{0} \end{pmatrix}, \begin{pmatrix} \Sigma & \mathbf{0} \\ \mathbf{0} & \Omega \end{pmatrix} \right). \quad (3)$$

Because  $M$  is selected from the observed data, inference must be performed based on the above distribution while conditioning on the selection event.

## 2.2 Selection-adjusted distribution

To characterize the conditional distribution of  $(\hat{\beta}_M, \omega) \mid \{\widehat{M} = M\}$ , we first study the selection event  $\{\widehat{M} = M\}$ . Here, we use  $\widehat{M}$  to denote the random variable of the model selected by the lasso problem (1), and use  $M$  to denote the realization of  $\widehat{M}$  on the observed data. Recall that the Karush-Kuhn-Tucker (KKT) condition for problem (1) is given by

$$\begin{aligned} X^\top (X \hat{\beta}^\lambda - Y) + \mathbf{s} &= \omega \\ \mathbf{s}_M &= \lambda \cdot \text{sign}(\hat{\beta}_M^\lambda), \quad \|\mathbf{s}_{-M}\|_\infty \leq \lambda. \end{aligned}$$

Here,  $\mathbf{s}$  denotes the subgradient of the penalty  $\lambda \|\beta\|_1$  at the solution  $\hat{\beta}^\lambda$ . By rearranging, we have

$$\begin{aligned} \omega &= X^\top X_M \hat{\beta}_M^\lambda - X^\top X_M \hat{\beta}_M + X^\top (X_M \hat{\beta}_M - Y) + \mathbf{s} \\ &= X^\top X_M D \mathbf{b} - X^\top X_M \hat{\beta}_M + \mathbf{r} + \mathbf{s}, \end{aligned} \quad (4)$$

where  $D = \text{diag}(\text{sign}(\hat{\beta}_M^\lambda))$  is the diagonal matrix of the signs of  $\hat{\beta}_M^\lambda$ ,  $\mathbf{b} = D \hat{\beta}_M^\lambda$  is the absolute value of  $\hat{\beta}_M^\lambda$ , and  $\mathbf{r} = X^\top (X_M \hat{\beta}_M - Y)$  represents the residual. If we condition not only on the selection event but also on the sign of the lasso solution  $\hat{\beta}_M^\lambda$  and the residual  $\mathbf{r}$ , then Equation (4) provides a one-to-one linear mapping from  $(\hat{\beta}_M, \omega)$  to  $(\hat{\beta}_M, \mathbf{b}, \mathbf{s}_{-M})$ :

$$\omega = Q_1 \hat{\beta}_M + Q_2 \mathbf{b} + \mathbf{r} + \mathbf{s}, \quad (5)$$

where  $Q_1 = -X^\top X_M$ ,  $Q_2 = X^\top X_M D$ ,  $\mathbf{r}$ , and  $\mathbf{s}_M$  are all constants when conditioned on  $\{\mathbf{r}, \mathbf{s}_M\}$ . Recall that the unconditional distribution of  $(\hat{\beta}_M, \omega)$  is the product Gaussian distribution given in Equation (3). Additionally, the KKT condition implies that  $\mathbf{b}$  is componentwise positive and  $\|\mathbf{s}_{-M}\|_\infty \leq \lambda$ . By applying this change-of-variable to the conditional distribution of  $(\hat{\beta}_M, \omega) \mid \{\mathbf{r}, \mathbf{s}_{-M}\}$ , we obtain the conditional density of  $(\hat{\beta}_M, \mathbf{b}, \mathbf{s}_{-M}) \mid \{\mathbf{r}, \mathbf{s}_M\}$ :

$$p(\hat{\beta}_M, \mathbf{b}, \mathbf{s}_{-M} \mid \{\mathbf{r}, \mathbf{s}_M\}) \propto \varphi(\hat{\beta}_M; \beta_M, \Sigma) \cdot \varphi(Q_1 \hat{\beta}_M + Q_2 \mathbf{b} + \mathbf{r} + \mathbf{s}; \mathbf{0}, \Omega) \cdot \mathbf{1}\{\mathbf{b} > \mathbf{0}, \|\mathbf{s}_{-M}\|_\infty \leq \lambda\}.$$

Lastly, we condition on  $\mathbf{s}_{-M}$  and marginalize over  $\mathbf{b}$  to obtain the conditional density of  $\hat{\beta}_M \mid \{\mathbf{r}, \mathbf{s}\}$ :

$$p(\hat{\beta}_M \mid \{\mathbf{r}, \mathbf{s}\}) = \frac{\varphi(\hat{\beta}_M; \beta_M, \Sigma) \cdot \int_{\mathbf{b} \in \mathcal{O}} \varphi(Q_1 \hat{\beta}_M + Q_2 \mathbf{b} + \mathbf{r} + \mathbf{s}; \mathbf{0}, \Omega) d\mathbf{b}}{\int_{\mathbb{R}^d} \varphi(\hat{\beta}_M; \beta_M, \Sigma) \cdot \int_{\mathbf{b} \in \mathcal{O}} \varphi(Q_1 \hat{\beta}_M + Q_2 \mathbf{b} + \mathbf{r} + \mathbf{s}; \mathbf{0}, \Omega) d\mathbf{b} d\hat{\beta}_M}, \quad (6)$$

where  $\mathcal{O} = \{\mathbf{v} \in \mathbb{R}^d : \mathbf{v} > \mathbf{0}\}$  represents the positive orthant in  $\mathbb{R}^d$ . We will see later that, with certain choice of the covariance matrix  $\Omega$  of the randomization variable, the above distribution is independent of  $\mathbf{r}_{-M}$  and  $\mathbf{s}_{-M}$ . Thus conditioning on  $\{\mathbf{r}_{-M}, \mathbf{s}_{-M}\}$  is not necessary.

In the following, we denote  $\mathcal{E} = \sigma(\{\mathbf{r}, \mathbf{s}\})$  as the  $\sigma$ -algebra generated by the random variables  $\mathbf{r}$  and  $\mathbf{s}$ . Before describing methods for conducting inference for  $\beta_M$  based on this conditional distribution, it is worth noting that data carving is asymptotically equivalent to the lasso with added noise as expressed in problem (1).

**Remark 2.1.** Initially proposed in [Fithian et al. \(2014\)](#), data carving refers to the approach that employs a subset of data for selection and uses the remaining information along with the hold-out data for inference. Specifically, this approach takes a subset of data  $(X^{(1)}, Y^{(1)})$  comprising  $n_1 < n$  observations and solves the lasso problem

$$\hat{\beta}^\lambda = \operatorname{argmin}_{\beta \in \mathbb{R}^p} \frac{1}{2\rho} \|Y^{(1)} - X^{(1)}\beta\|_2^2 + \lambda \|\beta\|_1,$$

where  $\rho = n_1/n \in (0, 1)$ . This problem can be expressed in the form as Problem (1), with the randomization variable defined as

$$\omega = -X^\top(Y - X\hat{\beta}^\lambda) + \frac{1}{\rho} X^{(1)\top}(Y^{(1)} - X^{(1)}\hat{\beta}^\lambda),$$

Moreover, as  $n \rightarrow \infty$  and  $n_1/n \rightarrow \rho$  and with fixed  $p$ ,  $\omega$  can be shown to have the asymptotic distribution  $\mathcal{N}(\mathbf{0}, \frac{1-\rho}{\rho} \sigma^2 X^\top X)$ . See [Markovic and Taylor \(2016\)](#) and [Liu and Panigrahi \(2023\)](#) for the asymptotic justification in the context of linear and generalized linear models. Hence, data carving is asymptotically equivalent to the randomized lasso problem in (1) with  $\Omega = \frac{1-\rho}{\rho} \sigma^2 X^\top X$ .

### 2.3 CDF-based inference

We focus on conducting inference for linear contrasts of the form  $\boldsymbol{\eta}^\top \beta_M$  for some  $\boldsymbol{\eta} \in \mathbb{R}^d$ . For testing the null hypothesis  $H_0 : \boldsymbol{\eta}^\top \beta_M = \theta$ , a valid p-value can be obtained by considering the tail probability of the observed value of  $\hat{\theta} := \boldsymbol{\eta}^\top \hat{\beta}_M$  within the conditional distribution given by Equation (6). To eliminate the nuisance parameters in  $\beta_M$ , we condition further on  $\beta^\perp := \hat{\beta}_M - \mathbf{c}\hat{\theta}$ , where  $\mathbf{c} = \nu^{-1} \Sigma \boldsymbol{\eta}$ ,  $\nu = \boldsymbol{\eta}^\top \Sigma \boldsymbol{\eta}$ .

Let  $\mathbf{t} = \mathbf{r} + \mathbf{s} + Q_1 \beta^\perp$ ,  $\tilde{Q}_1 = Q_1 \mathbf{c}$ . Then the KKT map in Equation (5) can be expressed as

$$\omega = \tilde{Q}_1 \hat{\theta} + Q_2 \mathbf{b} + \mathbf{t}.$$

Similar to Equation (6), the conditional density of  $\hat{\theta}$  given  $\{\mathcal{E}, \beta^\perp\}$  can be expressed as

$$\frac{\varphi(\hat{\theta}; \theta, \nu) \cdot \int_{\mathbf{b} \in \mathcal{O}} \varphi(\tilde{Q}_1 \hat{\theta} + Q_2 \mathbf{b} + \mathbf{t}; \mathbf{0}, \Omega) d\mathbf{b}}{\int_{\mathbb{R}} \varphi(\hat{\theta}; \theta, \nu) \cdot \int_{\mathbf{b} \in \mathcal{O}} \varphi(\tilde{Q}_1 \hat{\theta} + Q_2 \mathbf{b} + \mathbf{t}; \mathbf{0}, \Omega) d\mathbf{b} d\hat{\theta}}.$$

The CDF of the above distribution can serve as a one-sided p-value. The following proposition provides an expression of the CDF. Define  $H = Q_2^\top \Omega^{-1} Q_2$ ,  $\mathbf{k} = Q_2^\top \Omega^{-1} \mathbf{t}$ ,  $\tilde{\mathbf{c}} = D\mathbf{c}$ .

**Proposition 2.1** (CDF of  $\hat{\theta} \mid \{\mathcal{E}, \beta^\perp\}$ ). Under  $H_0 : \boldsymbol{\eta}^\top \boldsymbol{\beta}_M = \theta$ , the CDF  $F(x)$  of the distribution of  $\hat{\theta}$  conditional on  $\{\mathcal{E}, \beta^\perp\}$  is given by

$$F(x) = \frac{\int_{\mathbf{b} \in \mathcal{O}} \Phi\left(\frac{x - \mu_{\hat{\theta}}(\mathbf{b})}{\sigma_{\hat{\theta}}}\right) \varphi(\mathbf{b}; \boldsymbol{\mu}_{\mathbf{b}}, \Sigma_{\mathbf{b}}) d\mathbf{b}}{\int_{\mathbf{b} \in \mathcal{O}} \varphi(\mathbf{b}; \boldsymbol{\mu}_{\mathbf{b}}, \Sigma_{\mathbf{b}}) d\mathbf{b}}, \quad (7)$$

where

$$\begin{aligned} \Sigma_{\mathbf{b}}(\boldsymbol{\eta}) &= H^{-1} + \nu \tilde{\mathbf{c}} \tilde{\mathbf{c}}^\top, & \Sigma_{\mathbf{b}}(\boldsymbol{\eta})^{-1} \boldsymbol{\mu}_{\mathbf{b}}(\boldsymbol{\eta}) &= -\mathbf{k} + \sigma_{\hat{\theta}}^2 H \tilde{\mathbf{c}} (\nu^{-1} \theta + \tilde{\mathbf{c}}^\top \mathbf{k}), \\ \sigma_{\hat{\theta}}^2 &= (\nu^{-1} + \tilde{\mathbf{c}}^\top H \tilde{\mathbf{c}})^{-1}, & \sigma_{\hat{\theta}}^{-2} \mu_{\hat{\theta}}(\mathbf{b}) &= \nu^{-1} \theta + \tilde{\mathbf{c}}^\top \mathbf{k} + \tilde{\mathbf{c}}^\top H \mathbf{b}. \end{aligned}$$

See Appendix A.1 for the derivation. The derivation involves decomposing the joint distribution of  $(\hat{\theta}, \mathbf{b})$  into the conditional distribution of  $\hat{\theta} \mid \mathbf{b}$ , which is  $\mathcal{N}(\mu_{\hat{\theta}}(\mathbf{b}), \sigma_{\hat{\theta}}^2)$ , and the marginal distribution of  $\mathbf{b}$ , which is  $\mathcal{N}(\boldsymbol{\mu}_{\mathbf{b}}(\boldsymbol{\eta}), \Sigma_{\mathbf{b}}(\boldsymbol{\eta}))$ .

Note that the conditional variance  $\sigma_{\hat{\theta}}^2$  and conditional mean  $\mu_{\hat{\theta}}(\mathbf{b})$  of  $\hat{\theta}$  given  $\mathbf{b}$  also depend on  $\boldsymbol{\eta}$ , but we omit this dependence for simplicity of notation. Moreover, the expressions of  $\boldsymbol{\mu}_{\mathbf{b}}(\boldsymbol{\eta})$  and  $\mu_{\hat{\theta}}(\mathbf{b})$  depend on  $\mathbf{t}$ , which encompasses the random variables that are conditioned on. These expressions also depend on the value of  $\theta$ . However, the variances  $\Sigma_{\mathbf{b}}(\boldsymbol{\eta})$  and  $\sigma_{\hat{\theta}}^2$  remain unaffected by  $\mathbf{t}$  or  $\theta$ .

Recall from Remark 2.1 that data carving can be viewed as Problem (1) with the covariance of  $\boldsymbol{\omega}$  equal to  $\frac{1-\rho}{\rho} \sigma^2 X^\top X$ . In this special case, the CDF  $F(x)$  in Proposition 2.1 does not depend on  $\mathbf{t}_{-M}$  and the expression can be simplified.

**Corollary 2.2** ( $\Omega = \kappa^{-1} \cdot \sigma^2 X^\top X$ ). If  $\Omega = \kappa^{-1} \cdot \sigma^2 X^\top X$ , then  $\mathbf{k} = Q_2^\top \Omega^{-1} \mathbf{t} = (\kappa/\sigma^2) D \mathbf{t}_M$ . Consequently, the CDF in Proposition 2.1 does not depend on  $\mathbf{t}_{-M}$ . Moreover, we have the simplified expressions

$$\begin{aligned} \Sigma_{\mathbf{b}}(\boldsymbol{\eta}) &= H^{-1} + \nu \tilde{\mathbf{c}} \tilde{\mathbf{c}}^\top, & \boldsymbol{\mu}_{\mathbf{b}}(\boldsymbol{\eta}) &= -H^{-1} \mathbf{k} + \tilde{\mathbf{c}} \theta, \\ \sigma_{\hat{\theta}}^2 &= \frac{\nu}{1 + \kappa}, & \mu_{\hat{\theta}}(\mathbf{b}) &= \frac{\nu}{1 + \kappa} \left( \frac{\theta}{\nu} + \frac{\kappa}{\sigma^2} \tilde{\mathbf{c}}^\top \mathbf{t}_M + \frac{\kappa}{\nu} \boldsymbol{\eta}^\top D \mathbf{b} \right). \end{aligned}$$

This corollary indicates that when  $\Omega$  is a multiple of  $X^\top X$ , as is the case for data carving, the conditional distribution of  $\hat{\theta}$  becomes independent of  $\mathbf{s}_{-M}$  and  $\mathbf{r}_{-M}$ . In essence, it is equivalent to the distribution that is not conditioned on  $\mathbf{s}_{-M}$  and  $\mathbf{r}_{-M}$ . Consequently, choosing the randomization covariance matrix  $\Omega$  to be a multiple of  $X^\top X$  effectively reduces the conditioning set from  $\{\mathbf{s}, \mathbf{r}, \hat{\beta}^\perp\}$  to  $\{\mathbf{s}_M, \mathbf{r}_M, \hat{\beta}^\perp\}$ .

The CDF in Equation (7), evaluated at the observed value of  $\hat{\theta}$ , is a valid p-value since  $F(\hat{\theta}) \sim \text{Unif}([0, 1])$  conditional on  $\{\widehat{M} = M\}$ . Similarly,  $1 - F(\hat{\theta})$  and  $2 \cdot \min\{F(\hat{\theta}), 1 - F(\hat{\theta})\}$  are also uniformly distributed when conditioned on  $\{\widehat{M} = M\}$ . Consequently, they can be used to test the hypothesis  $H_0 : \boldsymbol{\eta}^\top \boldsymbol{\beta}_M = \theta$ . However, it is challenging to evaluate the CDF in Equation (7) due to the integral over  $\mathbf{b} \in \mathcal{O}$ . In fact, the CDF can be equivalently expressed as  $F(x) = \mathbb{E} \left[ \Phi\left(\frac{x - \mu_{\hat{\theta}}(\mathbf{b})}{\sigma_{\hat{\theta}}}\right) \right]$ , where the expectation is taken over  $\mathbf{b} \sim \mathcal{N}(\boldsymbol{\mu}_{\mathbf{b}}, \Sigma_{\mathbf{b}}) \mid_{\mathcal{O}}$ , the normal distribution truncated to the positive orthant. The main objective of this study is to provide a numerical integration algorithm to compute this expectation efficiently.

## 2.4 MLE-based inference

Aside from the CDF-based approach, another method for inference hinges on the approximate normality of the MLE of the selective likelihood. The following proposition provides an expression of the selective likelihood, derived from the selection-adjusted distribution of  $\hat{\beta}_M$ .

**Proposition 2.3** (Selective likelihood). *The conditional density in Equation (6) yields the selective likelihood up to a constant:*

$$\ell(\beta_M) = \frac{\varphi(\hat{\beta}_M; \beta_M, \Sigma)}{\int_{\mathbf{b} \in \mathcal{O}} \varphi(\mathbf{b}; \mu_{\mathbf{b}}, \Sigma_{\mathbf{b}}) d\mathbf{b}},$$

where

$$\Sigma_{\mathbf{b}} = H^{-1} + D\Sigma D, \quad \mu_{\mathbf{b}}(\beta_M) = D\beta_M - H^{-1}Q_2^T\Omega^{-1}(\mathbf{r} + \mathbf{s}).$$

The numerator of the selective likelihood corresponds to the unconditional density of  $\hat{\beta}_M$ , which mirrors the standard likelihood without any adjustments. The denominator arises from the normalizing constant of the density in Equation (6), which is equal to the probability of selecting the model. See the derivation in Appendix A.2.

The selective MLE  $\hat{\beta}^{\text{sMLE}}$  is thus the maximum of the likelihood function  $\ell(\beta_M)$ . Panigrahi and Taylor (2022) demonstrate that the distribution of  $\hat{\beta}^{\text{sMLE}}$  can be approximated by the normal distribution  $\mathcal{N}(\beta_M, (I^{\text{sMLE}})^{-1})$ , where  $I^{\text{sMLE}} = -\nabla^2 \log \ell(\hat{\beta}^{\text{sMLE}})$  is the Hessian of the negative logarithm of the selective likelihood at  $\hat{\beta}^{\text{sMLE}}$ . Given  $\hat{\beta}^{\text{sMLE}}$  and  $I^{\text{sMLE}}$ , a level- $(1 - \alpha)$  confidence interval for  $\eta^\top \beta_M$  can be constructed as

$$\eta^\top \hat{\beta}_M \pm q_{1-\alpha/2} \sqrt{\eta^\top (I^{\text{sMLE}})^{-1} \eta},$$

where  $q_{1-\alpha/2} = \Phi^{-1}(1 - \alpha/2)$  is the  $(1 - \alpha/2)$  quantile of the standard normal distribution. The advantage of this approach is that it avoids the need to condition on  $\beta^\perp$  to eliminate nuisance parameters, which is required in the CDF-based inference. A limitation of this method is that the distribution of  $\hat{\beta}^{\text{sMLE}}$  is approximated as a Gaussian distribution, rather than being exactly Gaussian. For example, the Gaussian approximation might perform poorly in cases where the randomization level is weak, as shown by Panigrahi and Taylor (2022).

Panigrahi and Taylor (2022) propose an approximate method to find the selective MLE and its corresponding Fisher information. Their method relies on a large deviation approximation of the selection probability, which can lead to unreliable results if this approximation is not accurate. In this work, we provide an algorithm to compute the MLE and Fisher information more precisely.

## 2.5 Related work

In the literature of conditional post-selection inference, the conditional distributions similar to the one in Equation (6) are often handled by MCMC sampling, such as Gibbs sampling (Tian et al., 2016), hit-and-run (Bélisle et al., 1993; Fithian et al., 2014; Tian et al., 2018), and projected Langevin dynamics (Markovic and Taylor, 2016). The substantial computational demands of these MCMC-based methods is the main motivation for the development of the more efficient sampling algorithm in this work.

Several sampling-free methods have been specifically designed for the randomized lasso. The approximate MLE method by Panigrahi and Taylor (2022) mentioned earlier is one example. Panigrahi et al. (2022) propose a method that involves further conditioning to make the conditional distribution tractable, enabling the derivation of exact p-values and confidence intervals. However, this “over-conditioning” could potentially diminish statistical power. A comparative evaluation of these methods is conducted in simulation in Section 5.

A common criticism of randomized selection algorithms revolves around the variability in the selected model due to different realizations of randomness. To address this concern, Schultheiss et al. (2021) propose to perform multicarving across multiple partitions of the data to enhance robustness and reproducibility. However, this approach requires MCMC sampling for every single carving and every single parameter, thereby restricting its practicality. In this context, our proposed method can play a crucial role in reducing the computational demands of multicarving.

Post-selection inference with more complex data or selection algorithms is an active area of research. Liu and Panigrahi (2023) develop an algorithm for post-selection inference with distributed data, where model selection is performed locally and only summary statistics are communicated to deliver inference for the aggregated model. Liu et al. (2022) propose a generic approach for inference after a general model selection. Their approach heavily relies on the assumption that the selection procedure can be repeatedly executed on bootstrapped datasets in order to acquire knowledge about the selection event.

Beyond the conditional approach, the PoSI framework introduced by Berk et al. (2013) and extended by Bachoc et al. (2019, 2020); Kuchibhotla et al. (2020) provides simultaneous inference that guarantees validity across all selection procedures. Consequently, these methods can be conservative due to their worst-case guarantee.

More recently, Rasines and Young (2021) propose a splitting strategy that mimics sample splitting, but the information splitting is conducted via added Gaussian noise. This method, termed the  $(U, V)$  decomposition, involves generating a Gaussian vector  $W$  such that  $U = Y + \gamma W$  is independent of  $V = Y - \gamma^{-1}W$ . Model selection is carried out on  $U$  while inference is conducted on  $V$ . Due to the independence between  $U$  and  $V$ , the inference is free of selection bias. Leiner et al. (2021) generalize this approach to settings where the data is not necessarily Gaussian and name their approach “data fission”.

### 3 Separation-of-variable method

In this section, we will describe the proposed method for computing the CDF  $F(x)$  for some fixed  $x \in \mathbb{R}$  in Equation (7). For simplicity, we will denote  $\boldsymbol{\mu} = \boldsymbol{\mu}_{\mathbf{b}}$ ,  $\Sigma = \Sigma_{\mathbf{b}}$ , as well as

$$\mathbf{g}_1 = -\sigma_{\hat{\theta}} H \tilde{\mathbf{c}}, \quad g_2 = \frac{x}{\sigma_{\hat{\theta}}} - \sigma_{\hat{\theta}} (\nu^{-1} \theta + \tilde{\mathbf{c}}^\top \mathbf{k})$$

such that  $\mathbf{g}_1^\top \mathbf{b} + g_2 = \frac{1}{\sigma_{\hat{\theta}}} (x - \mu_{\hat{\theta}}(\mathbf{b}))$ . With this notation,  $F(x)$  can be expressed as

$$F(x) = \frac{\int_{\mathbf{b} \in \mathcal{O}} \Phi(\mathbf{g}_1^\top \mathbf{b} + g_2) \varphi(\mathbf{b}; \boldsymbol{\mu}, \Sigma) d\mathbf{b}}{\int_{\mathbf{b} \in \mathcal{O}} \varphi(\mathbf{b}; \boldsymbol{\mu}, \Sigma) d\mathbf{b}}. \quad (8)$$

We begin by observing that the denominator of Equation (8) is equal to the orthant probability of the distribution  $\mathcal{N}(\boldsymbol{\mu}, \Sigma)$ . The most widely-used method to compute this orthant probability is



the separation-of-variable (SOV) technique introduced by Genz (1992). The SOV method starts by reparameterizing  $\mathbf{b}$  as  $\mathbf{b} = L\mathbf{z} + \boldsymbol{\mu}$ , where  $L$  is the Cholesky decomposition of  $\Sigma$  and  $\mathbf{z} \sim \mathcal{N}(0, I) |_{L\mathbf{z} + \boldsymbol{\mu} \in \mathcal{O}}$ . This enables us to express  $F(x)$  equivalently as

$$F(x) = \frac{\int_{L\mathbf{z} + \boldsymbol{\mu} \in \mathcal{O}} \Phi(\tilde{\mathbf{g}}_1^\top \mathbf{z} + \tilde{g}_2) \varphi(\mathbf{z}) d\mathbf{z}}{\int_{L\mathbf{z} + \boldsymbol{\mu} \in \mathcal{O}} \varphi(\mathbf{z}) d\mathbf{z}}, \quad \text{where } \tilde{\mathbf{g}}_1 = L^\top \mathbf{g}_1, \tilde{g}_2 = g_2 + \mathbf{g}_1^\top \boldsymbol{\mu}.$$

Because  $L$  is lower-triangular and has positive diagonals, i.e.  $L_{kk} > 0$  for all  $k$ , the constraint of  $L\mathbf{z} + \boldsymbol{\mu} \in \mathcal{O}$ , which is  $\mu_k + \sum_{j=1}^k L_{kj} z_j > 0 \forall k \in [d]$ , can be sequentially expressed out for each variable  $k = 1, 2, \dots, d$  as follows:

$$z_k \geq \frac{-\mu_k - \sum_{j=1}^{k-1} L_{kj} z_j}{L_{kk}} =: a_k(\mathbf{z}_{1:k-1}).$$

The value of  $a_k$  depends on the realization of the previous  $k-1$  variables  $\mathbf{z}_{1:k-1}$ , and serves as the lower bound of  $z_k$  in the spherical Gaussian space. Consequently, the denominator is equal to

$$\begin{aligned} \int_{L\mathbf{z} + \boldsymbol{\mu} \in \mathcal{O}} \varphi(\mathbf{z}) d\mathbf{z} &= \int_{z_1 \geq a_1} \varphi(z_1) \int_{z_2 \geq a_2(z_1)} \varphi(z_2) \cdots \int_{z_d \geq a_d(\mathbf{z}_{1:d-1})} \varphi(z_d) d\mathbf{z} \\ &= \int_{\Phi(a_1)}^1 \int_{\Phi(a_2)}^1 \cdots \int_{\Phi(a_d)}^1 d\mathbf{v} \quad (\text{where } v_k = \Phi(z_k)) \\ &= \int_{[0,1]^d} \prod_{k=1}^d (1 - \Phi(a_k)) d\mathbf{u} \quad (\text{where } v_k = \Phi(a_k) + (1 - \Phi(a_k))u_k) \end{aligned}$$

where the second equality applies the change-of-variable  $z_k = \Phi^{-1}(v_k)$  and the third equality shifts and scales the variables  $v_k$  so that the integral is over the unit cube  $[0, 1]^d$ . These transformations establish the relationships among  $\mathbf{u}$ ,  $\mathbf{a}$ ,  $\mathbf{z}$  as

$$a_k = \frac{-\mu_k - \sum_{j=1}^{k-1} L_{kj} z_j}{L_{kk}}, \quad z_k = \Phi^{-1}(\Phi(a_k) + u_k(1 - \Phi(a_k))), \quad \forall 1 \leq k \leq d. \quad (9)$$

Throughout the rest of the paper, these dependencies should always be understood, even if not explicitly stated. In addition, we always assume  $\mathbf{b} = L\mathbf{z} + \boldsymbol{\mu}$ .

Analogously, the numerator  $\int_{L\mathbf{z} + \boldsymbol{\mu} \in \mathcal{O}} \Phi(\tilde{\mathbf{g}}_1^\top \mathbf{z} + \tilde{g}_2) \varphi(\mathbf{z}) d\mathbf{z}$  can also be expressed as the integral

$$\int_{[0,1]^d} \Phi(\tilde{\mathbf{g}}_1^\top \mathbf{z} + \tilde{g}_2) \prod_{k=1}^d (1 - \Phi(a_k)) d\mathbf{u},$$

where  $\mathbf{z}$ ,  $\mathbf{a}$  also satisfy Equation (9). We define the SOV weight  $w(\mathbf{u})$  as the function

$$w(\mathbf{u}) = \prod_{k=1}^d (1 - \Phi(a_k)), \quad (10)$$

with the understanding that the dependence of  $a_k$  on  $\mathbf{u}$  is implied by Equation (9). This leads us to the expression

$$F(x) = \frac{\int_{[0,1]^d} \Phi(\tilde{\mathbf{g}}_1^\top \mathbf{z} + \tilde{g}_2) w(\mathbf{u}) d\mathbf{u}}{\int_{[0,1]^d} w(\mathbf{u}) d\mathbf{u}}. \quad (11)$$

This expression allows us to estimate  $F(x)$  by generating uniform samples  $\mathbf{u}^{(1)}, \dots, \mathbf{u}^{(N)}$  in the unit cube  $[0, 1]^d$  and computing

$$\widehat{F(x)} = \frac{\frac{1}{N} \sum_{i=1}^N \Phi(\tilde{\mathbf{g}}_1^\top \mathbf{z}^{(i)} + \tilde{g}_2) w(\mathbf{u}^{(i)})}{\frac{1}{N} \sum_{i=1}^N w(\mathbf{u}^{(i)})}, \quad (12)$$

where each  $\mathbf{z}^{(i)}$  is determined by  $\mathbf{u}^{(i)}$  via Equation (9). It is worth noting that this estimator is equivalent to the self-normalized importance sampling (SNIS) estimator using proposal density

$$\prod_{k=1}^d \frac{\varphi(z_k) \mathbf{1}\{z_k \geq a_k(\mathbf{z}_{1:k-1})\}}{1 - \Phi(a_k(\mathbf{z}_{1:k-1}))},$$

since the ratio between  $\varphi(\mathbf{z}) \mathbf{1}\{L\mathbf{z} + \boldsymbol{\mu} \in \mathcal{O}\}$  and the above proposal density is exactly equal to the SOV weight  $w(\mathbf{u})$ .

### 3.1 Variance reduction

In order to enhance the precision of the Monte Carlo estimator in Equation (12), we can employ several variance reduction techniques.

**Conditional Monte Carlo** First, we observe that the denominator of the quantity given in Equation (11) is in fact a  $(d-1)$ -dimensional integral. This is because  $a_k$  only depends on  $\mathbf{u}_{1:k-1}$ , thus the SOV weight  $w(\mathbf{u}) = \prod_{k=1}^d (1 - \Phi(a_k))$  does not depend on  $u_d$ . If the numerator can also be evaluated using  $\mathbf{u}_{1:d-1}$  only, then it suffices to sample from the  $(d-1)$ -dimensional unit cube instead of the  $d$ -dimensional unit cube.

To achieve this, we will integrate out  $u_d$  from the integrand in the numerator exactly. This technique is known as conditional Monte Carlo, or pre-integration, or Rao-Blackwellization (Blackwell, 1947; Casella and Robert, 1996). By integrating out some variable in a closed form, we always reduce the Monte Carlo variance of the estimator. Note that the integrand in the numerator is given by  $\Phi(\tilde{\mathbf{g}}_1^\top \mathbf{z} + \tilde{g}_2) \prod_{k=1}^d (1 - \Phi(a_k))$ . Integrating out  $u_d$  can be carried out as follows:

$$\begin{aligned} & \int_0^1 \Phi(\tilde{g}_{1,d} z_d + \tilde{\mathbf{g}}_{1,-d}^\top \mathbf{z}_{-d} + \tilde{g}_2) \prod_{k=1}^d (1 - \Phi(a_k)) du_d \\ &= \prod_{k=1}^{d-1} (1 - \Phi(a_k)) \cdot \int_{a_d}^{\infty} \Phi(\tilde{g}_{1,d} z_d + \tilde{\mathbf{g}}_{1,-d}^\top \mathbf{z}_{-d} + \tilde{g}_2) \varphi(z_d) dz_d. \end{aligned}$$

The above univariate integral can be expressed as the CDF of a bivariate normal distribution, which can be evaluated efficiently with high precision based on Owen's T function (Patefield, 2000).

**Variable reordering** The SOV estimator's performance depends on the arrangement of the variables. As noted in Genz (1992), rearranging variables might lead to significant error reduction when computing the Gaussian orthant probabilities. Gibson et al. (1994) introduced a heuristic method to reorder the variables so that the innermost integrals have the largest expected values. We apply the Gibson ordering to reorder the variables before employing the SOV method to compute the integrals.

**Quasi-Monte Carlo** The integrands  $w(\mathbf{u})$  and  $\Phi(\tilde{\mathbf{g}}_1^\top \mathbf{z} + \tilde{g}_2)w(\mathbf{u})$  are bounded and smooth on the unit cube, making them highly suitable for quasi-Monte Carlo (QMC) sampling. If the points  $\mathbf{u}^{(i)}$  ( $1 \leq i \leq N$ ) are sampled uniformly and independently in the unit cube, then the estimator in Equation (12) has a probabilistic error rate of  $O_p(N^{-1/2})$  for both the numerator and the denominator separately. This error rate can be substantially improved by adopting QMC or randomized QMC (RQMC) methods. QMC points are chosen strategically and deterministically to cover the unit cube more evenly than i.i.d. Monte Carlo does. For integrands of bounded variation in the sense of Hardy-Krause, QMC achieves an error rate of  $O(N^{-1+\delta})$  for any  $\delta > 0$ , where  $N^\delta$  hides the the log term  $(\log N)^d$  (Niederreiter, 1992).

However, this error rate is obtained by a worst-case upper bound and is often too conservative to be useful as an error estimate. Moreover, it does not apply for functions with unbounded Hardy-Krause variation. One remedy to these issues is to apply randomization. In RQMC, the points  $\mathbf{u}^{(i)}$  are uniformly distributed individually while collectively they have the low-discrepancy property of QMC. This ensures that the estimator of the integral is unbiased, and its standard error can be estimated by independent replicates. Randomization can be achieved by adding a random shift to lattice rules or by randomly scrambling the digits of digital nets. See L'Ecuyer and Lemieux (2002) for a review of RQMC.

In this work, we propose to use scrambled Sobol' points (Sobol', 1967; Owen, 1995), a particular type of RQMC points. These points are construction-free, thereby eliminating the need for case-by-case constructions as required by lattice rules. For sufficiently smooth integrands, it can achieve an error rate of  $O(N^{-3/2+\delta})$  (Owen, 1997a,b). In addition, it has been observed by Hong and Hickernell (2003) that scrambled Sobol' points perform empirically better than competing methods for this particular problem of computing multivariate normal probabilities.

### 3.2 Confidence intervals

In practice, there might be a need to test the hypothesis  $\boldsymbol{\eta}^\top \boldsymbol{\beta}_M = \theta$  for a range of different values of  $\theta$  and  $\boldsymbol{\eta}$ . For instance, we might want to test  $\beta_{M,j} = 0$  for all  $j \in M$ . Moreover, constructing a confidence interval for  $\boldsymbol{\eta}^\top \boldsymbol{\beta}_M$  involves inverting the hypothesis testing, requiring the computation of the pivotal quantity  $F(x)$  defined in Proposition 2.1 for various values of  $\theta$ . While we can apply the SOV method to compute p-values for each individual hypothesis separately, we offer an approach that facilitates testing the hypothesis  $\boldsymbol{\eta}^\top \boldsymbol{\beta}_M = \theta$  for any  $\boldsymbol{\eta}$  and  $\theta$  using just a single batch of RQMC samples.

Recall that when testing  $\boldsymbol{\eta}^\top \boldsymbol{\beta}_M = \theta$ , we require sampling  $\mathbf{b}$  from  $\mathcal{N}(\boldsymbol{\mu}_b(\boldsymbol{\eta}, \theta), \Sigma_b(\boldsymbol{\eta})) \mid \mathcal{O}$ , where

$$\begin{aligned}\Sigma_b(\boldsymbol{\eta})^{-1} &= H - \sigma_\theta^2 H \tilde{\mathbf{c}} \tilde{\mathbf{c}}^\top H, \\ \Sigma_b(\boldsymbol{\eta})^{-1} \boldsymbol{\mu}_b(\boldsymbol{\eta}, \theta) &= -\mathbf{k} + \sigma_\theta^2 H \tilde{\mathbf{c}} (\nu^{-1} \theta + \tilde{\mathbf{c}}^\top \mathbf{k}).\end{aligned}$$

according to Proposition 2.1. Here the notation emphasizes the dependence of  $\boldsymbol{\mu}_b$  and  $\Sigma_b$  on  $\boldsymbol{\eta}$  and  $\theta$ .

Rather than sampling from  $\mathcal{N}(\boldsymbol{\mu}_b(\boldsymbol{\eta}, \theta), \Sigma_b(\boldsymbol{\eta})) \mid \mathcal{O}$ , which depends on  $(\boldsymbol{\eta}, \theta)$ , we propose to sample from the distribution  $\mathcal{N}(\bar{\boldsymbol{\mu}}, \bar{\Sigma}) \mathbf{1}_{\{\mathcal{O}\}}$ , where

$$\begin{aligned}\bar{\Sigma}^{-1} &= H, \\ \bar{\Sigma}^{-1} \bar{\boldsymbol{\mu}} &= -Q_2^\top \Omega^{-1} (\mathbf{r} + \mathbf{s} - X^\top X_M \hat{\boldsymbol{\beta}}_M).\end{aligned}\tag{13}$$

This distribution is also supported on the orthant  $\mathcal{O}$  and is independent of  $(\boldsymbol{\eta}, \theta)$ . The underlying rationale for this choice is to achieve a proximity between  $(\bar{\Sigma}^{-1}, \bar{\Sigma}^{-1}\bar{\boldsymbol{\mu}})$  and  $(\Sigma_{\mathbf{b}}(\boldsymbol{\eta})^{-1}, \Sigma_{\mathbf{b}}(\boldsymbol{\eta})^{-1}\boldsymbol{\mu}_{\mathbf{b}}(\boldsymbol{\eta}, \theta))$  across different values of  $\boldsymbol{\eta}$  and  $\theta$ .

To evaluate integrals w.r.t. the target distribution  $\mathcal{N}(\boldsymbol{\mu}_{\mathbf{b}}(\boldsymbol{\eta}, \theta), \Sigma_{\mathbf{b}}(\boldsymbol{\eta})) |_{\mathcal{O}}$ , we apply importance weighting. The expression of the importance weight is given in the following lemma.

**Lemma 1** (Importance weight relative to  $\mathcal{N}(\bar{\boldsymbol{\mu}}, \bar{\Sigma}) |_{\mathcal{O}}$ ). *Given  $(\boldsymbol{\eta}, \theta)$ , let  $\mathbf{k}$ ,  $\tilde{\mathbf{c}}$  be as defined in Section 2.3. Define  $\Delta = \sigma_{\hat{\theta}}(\nu^{-1}\theta + \tilde{\mathbf{c}}^\top \mathbf{k} - \frac{\hat{\theta}}{\sigma_{\hat{\theta}}})$  and  $\boldsymbol{\tau} = \sigma_{\hat{\theta}} H \tilde{\mathbf{c}}$ . Then the importance weight  $\frac{\varphi(\mathbf{b}; \boldsymbol{\mu}_{\mathbf{b}}(\boldsymbol{\eta}, \theta), \Sigma_{\mathbf{b}}(\boldsymbol{\eta}))}{\varphi(\mathbf{b}; \bar{\boldsymbol{\mu}}, \bar{\Sigma})} \mathbf{1}_{\{\mathbf{b} \in \mathcal{O}\}}$  is proportional to*

$$\bar{w}(\mathbf{b}) := \exp \left[ \frac{1}{2} (\mathbf{b}^\top \boldsymbol{\tau})^2 + \Delta (\mathbf{b}^\top \boldsymbol{\tau}) \right] \mathbf{1}_{\{\mathbf{b} \in \mathcal{O}\}}. \quad (14)$$

See the derivation in Appendix A.3. Notably,  $\bar{w}(\mathbf{b})$  is a function of the inner product  $\mathbf{b}^\top \boldsymbol{\tau}$ . Thus, the computation of the importance weight requires only the evaluation of this vector-vector product, eliminating the need for matrix-vector products. Furthermore, this implies that the importance sampling effectively operates as a one-dimensional importance sampling, thereby circumventing the potential challenge related to products of weights in high dimensions.

Now we summarize the entire procedure. We first generate  $N$  samples  $\{\mathbf{u}^{(i)}\}_{1 \leq i \leq N}$  within the unit cube  $[0, 1]^d$  by RQMC. Then we apply the SOV method to obtain samples  $\{\mathbf{b}^{(i)}\}_{1 \leq i \leq N}$  from  $\mathcal{N}(\bar{\boldsymbol{\mu}}, \bar{\Sigma}) |_{\mathcal{O}}$  with the associated SOV weights  $\{w(\mathbf{u}^{(i)})\}_{1 \leq i \leq N}$ . For each sample  $\mathbf{b}^{(i)}$ , we calculate the importance weight  $\bar{w}(\mathbf{b}^{(i)})$  given by Equation (14) and then set  $w^{(i)} = w(\mathbf{u}^{(i)}) \cdot \bar{w}(\mathbf{b}^{(i)})$ . Then the weighted samples  $\mathbf{b}^{(i)}$ , weighted by  $w^{(i)}$ , are effectively drawn from  $\mathcal{N}(\boldsymbol{\mu}_{\mathbf{b}}(\boldsymbol{\eta}, \theta), \Sigma_{\mathbf{b}}(\boldsymbol{\eta})) |_{\mathcal{O}}$ . For a particular pair of  $\boldsymbol{\eta}$  and  $\theta$ , an estimate of the CDF  $F(x)$  defined in Equation (7) can be constructed similarly as Equation (12), with the weights being  $w^{(i)}$ . A valid one-sided p-value for testing  $\boldsymbol{\eta}^\top \boldsymbol{\beta}_M = \theta$  is obtained by evaluating  $F(x)$  (or  $1 - F(x)$ ) at the observed value of  $\boldsymbol{\eta}^\top \hat{\boldsymbol{\beta}}_M$ .

To construct a confidence for  $\boldsymbol{\eta}^\top \boldsymbol{\beta}_M$ , we need to invert the hypothesis tests for  $\boldsymbol{\eta}^\top \boldsymbol{\beta}_M = \theta$ . To achieve this, we vary  $\theta$  across a grid and form the interval of those values of  $\theta$  for which the corresponding hypothesis is not rejected. For instance, we can take a grid within the interval  $[\hat{\beta}_j^{(2)} - 10s_j, \hat{\beta}_j^{(2)} + 10s_j]$ , where  $\hat{\boldsymbol{\beta}}^{(2)}$  is the unbiased estimator of  $\boldsymbol{\beta}_M$  computed using the hold-out data only, and  $s_j$  is the corresponding standard error. Hence, the interval  $[\hat{\beta}_j^{(2)} - 10s_j, \hat{\beta}_j^{(2)} + 10s_j]$  most likely covers all the  $\theta$  that will not be rejected. The whole procedure is summarized in Algorithm 1.

## 4 MLE-based inference

This section describes how to maximize the selective likelihood given in Proposition 2.3 and conduct inference based on the MLE. The negative logarithm of the selective likelihood is equal to

$$-\log \ell(\boldsymbol{\beta}_M) = \frac{1}{2} (\hat{\boldsymbol{\beta}}_M - \boldsymbol{\beta}_M)^\top \Sigma^{-1} (\hat{\boldsymbol{\beta}}_M - \boldsymbol{\beta}_M) + \log \int_{\mathbf{b} \in \mathcal{O}} \varphi(\mathbf{b}; \boldsymbol{\mu}_{\mathbf{b}}(\boldsymbol{\beta}_M), \Sigma_{\mathbf{b}}) d\mathbf{b},$$

where  $\boldsymbol{\mu}_{\mathbf{b}}(\boldsymbol{\beta}_M)$  and  $\Sigma_{\mathbf{b}}$  are given in Proposition 2.3.

We propose to run gradient descent to minimize the negative log-likelihood  $-\log \ell(\boldsymbol{\beta}_M)$ . A challenge arises due to the presence of the orthant probability  $\int_{\mathbf{b} \in \mathcal{O}} \varphi(\mathbf{b}; \boldsymbol{\mu}_{\mathbf{b}}(\boldsymbol{\beta}_M), \Sigma_{\mathbf{b}}) d\mathbf{b}$  in the

---

**Algorithm 1** Confidence intervals for the components of  $\beta_M$  using the SOV method
 

---

Compute  $\bar{\mu}$  and  $\bar{\Sigma}$  defined in Equation (13).

Apply the SOV method with RQMC to get  $N$  weighted samples  $\{(\mathbf{b}^{(i)}, w(\mathbf{u}^{(i)}))\}_{i=1}^N$  from  $\mathcal{N}(\bar{\mu}, \bar{\Sigma})|_{\mathcal{O}}$ .

**for**  $j \leftarrow 1, \dots, d$  **do**

Let  $\boldsymbol{\eta} = \mathbf{e}_j$  and compute  $\mathbf{k}, \tilde{\mathbf{c}}$  as defined in Section 2.3. Compute  $\sigma_{\hat{\theta}}^2$  as in Proposition 2.1.

Let  $\hat{\beta}^{(2)}$  be the least-squares estimator of  $\beta_M$  using the hold-out data and let

$$s_j = \sigma \sqrt{[(X_M^{(2),\top} X_M^{(2)})^{-1}]_{jj}}.$$

Let  $\mathcal{G}$  be a grid on  $[\hat{\beta}_j^{(2)} - 10s_j, \hat{\beta}_j^{(2)} + 10s_j]$

**for**  $\theta$  in  $\mathcal{G}$  **do**

Compute  $\mu_{\hat{\theta}}(\mathbf{b}^{(i)})$  for  $1 \leq i \leq N$  as in Proposition 2.1 with the specific value of  $\theta$ .

Compute  $w^{(i)} = w(\mathbf{u}^{(i)}) \cdot \bar{w}(\mathbf{b}^{(i)})$ , where  $\bar{w}$  is defined in (14).

Compute the p-value by

$$p(\theta) = \frac{\sum_{i=1}^N \Phi\left(\frac{\hat{\beta}_{M,j} - \mu_{\hat{\theta}}(\mathbf{b}^{(i)})}{\sigma_{\hat{\theta}}}\right) w^{(i)}}{\sum_{i=1}^N w^{(i)}},$$

or  $1 - p(\theta)$  or  $2 \cdot \min\{p(\theta), 1 - p(\theta)\}$

**end for**

Form the confidence interval for  $\beta_{M,j}$  as  $\{\theta \in \mathcal{G} : p(\theta) \geq 1 - \alpha\}$ .

**end for**

**Output:** Level- $(1 - \alpha)$  confidence intervals for  $\beta_{M,j}$  ( $1 \leq j \leq d$ )

---

objective function. In our case, we need the gradient and Hessian of the log orthant probability w.r.t.  $\beta_M$ . Since the Jacobian of  $\boldsymbol{\mu}_{\mathbf{b}}(\beta_M)$  w.r.t.  $\beta_M$  is equal to  $D$ , it suffices if we can evaluate the gradient and Hessian of the log orthant probability w.r.t.  $\boldsymbol{\mu}_{\mathbf{b}}$ . The next lemma provides expressions for the gradient and the Hessian of the log orthant probability.

**Lemma 2** (Gradient and Hessian of log orthant probability). *Let  $h(\boldsymbol{\mu}) := \int_{\mathcal{O}} \varphi(\mathbf{b}; \boldsymbol{\mu}, \Sigma) d\mathbf{b}$  denote the orthant probability as a function of  $\boldsymbol{\mu}$ . Let  $\tilde{\boldsymbol{\mu}}$  and  $\tilde{\Sigma}$  denote the mean and covariance matrix of the truncated normal distribution  $\mathcal{N}(\boldsymbol{\mu}, \Sigma) |_{\mathcal{O}}$ . Then  $\nabla_{\boldsymbol{\mu}} \log h(\boldsymbol{\mu})$  and  $\nabla_{\boldsymbol{\mu}}^2 \log h(\boldsymbol{\mu})$  have the expressions*

$$\begin{aligned} \nabla_{\boldsymbol{\mu}} \log h(\boldsymbol{\mu}) &= \Sigma^{-1}(\tilde{\boldsymbol{\mu}} - \boldsymbol{\mu}), \\ \nabla_{\boldsymbol{\mu}}^2 \log h(\boldsymbol{\mu}) &= -\Sigma^{-1} + \Sigma^{-1} \tilde{\Sigma} \Sigma^{-1}. \end{aligned}$$

See the proof in the Appendix A.4. With the above lemma at hand, we can compute the gradient and Hessian of  $-\log \ell(\beta_M)$  as

$$\begin{aligned} -\nabla_{\beta_M} \log \ell(\beta_M) &= -\Sigma^{-1}(\hat{\beta}_M - \beta_M) + D \Sigma_{\mathbf{b}}^{-1}(\tilde{\boldsymbol{\mu}}_{\mathbf{b}} - \boldsymbol{\mu}_{\mathbf{b}}) \\ -\nabla_{\beta_M}^2 \log \ell(\beta_M) &= \Sigma^{-1} + D(\Sigma_{\mathbf{b}}^{-1} \tilde{\Sigma}_{\mathbf{b}} \Sigma_{\mathbf{b}}^{-1} - \Sigma_{\mathbf{b}}^{-1}) D, \end{aligned}$$

where  $\widetilde{\boldsymbol{\mu}}_{\mathbf{b}}$  and  $\widetilde{\Sigma}_{\mathbf{b}}$  are the mean and covariance of the truncated normal distribution  $\mathcal{N}(\boldsymbol{\mu}_{\mathbf{b}}(\boldsymbol{\beta}_M), \Sigma_{\mathbf{b}}) |_{\mathcal{O}}$ . The SOV method described in Section 3 can be used to efficiently evaluate the quantities  $\widetilde{\boldsymbol{\mu}}_{\mathbf{b}}$  and  $\widetilde{\Sigma}_{\mathbf{b}}$ . Therefore, we can run gradient descent using the SOV estimator of the gradient. After achieving convergence, we compute the Hessian matrix and conduct Wald-type inference the same as described in Section 2.4.

Note that the Hessian matrix  $-\nabla_{\boldsymbol{\beta}_M}^2 \log \ell(\boldsymbol{\beta}_M)$  is always positive definite because

$$\Sigma^{-1} \succeq D\Sigma_{\mathbf{b}}^{-1}D,$$

since  $D\Sigma_{\mathbf{b}}D = DH^{-1}D + \Sigma \succeq \Sigma$ . Consequently, the objective function is strongly convex, leading to linear convergence of the gradient descent algorithm. Even though we rely on a gradient estimate rather than the exact gradient in the gradient descent algorithm, this estimate proves to be surprisingly accurate even with a moderate number of RQMC samples. To further enhance the accuracy of the solution, one can consider increasing the number  $N$  of RQMC samples as the optimization process approaches the optimum.

## 5 Simulations

This section demonstrates the effectiveness of the proposed algorithm via simulations and real data analysis.

### 5.1 Carving for linear model

We adopt a similar experimental setup to the one used in Panigrahi and Taylor (2022). Specifically, we set  $n = 300$  and  $p = 100$ . The data are generated as  $\mathbf{x}_i \stackrel{iid}{\sim} \mathcal{N}(0, \Sigma_X)$  and  $y_i | \mathbf{x}_i \sim \mathcal{N}(x_i^\top \boldsymbol{\beta}, \sigma^2)$  where  $\sigma^2 = 1$ . Two types of covariance matrices  $\Sigma_X$  are considered: auto-regressive matrix (AR) with  $\Sigma_{ij} = 0.9^{|i-j|}$  and equi-correlation matrix (Equi) with  $\Sigma_{ij} = 0.9 + 0.1\mathbf{1}_{\{i=j\}}$ . The regression coefficient  $\boldsymbol{\beta}$  is designed to be a sparse vector with 10 nonzero coordinates, which are set to be  $\pm\sqrt{2c_0 \log(p)/n}$  with random signs and with  $c_0$  varied among  $\{0.6, 0.9, 1.2\}$ . We use 240 observations (i.e. 80% of the data) for the lasso variable selection, where the lasso regularization parameter  $\lambda$  is determined through two different approaches:

- $\lambda_{CV}$ : choosing  $\lambda$  based on a 5-fold cross-validation. Note that the selection of  $\lambda$  introduces additional bias but we did not correct for it. This choice is also considered in Schultheiss et al. (2021); Panigrahi and Taylor (2022).
- $\lambda_{\text{theory}}$ : setting  $\lambda = \sqrt{\log(p)/n_1}$ , as recommended by the theoretical result in Negahban et al. (2012). This choice of  $\lambda$  is also used by Panigrahi and Taylor (2022).

The objective is to construct 95% confidence intervals for each coordinate of the target  $X_M^\dagger X \boldsymbol{\beta}$  in the submodel view. The assessment is based on two key metrics: the average coverage probability, which denotes the proportion of confidence intervals that correctly cover the target parameters, and the average interval lengths. We consider the following inference methods:

- Splitting: Confidence intervals are constructed using only the remaining 20% of the data.

- Bivariate-normal: Panigrahi et al. (2022) propose to condition even further so that the conditional distribution of  $\hat{\theta}$  becomes tractable. Recall that our inference is based on the conditional distribution given in Equation (6), which marginalizes over the  $d$ -dimensional vector  $\mathbf{b}$ . To conduct inference for  $\beta_{M,j}$ , the method in Panigrahi et al. (2022) conditions on  $\mathbf{b}_{-j}$  so that the joint conditional distribution of  $(\hat{\beta}_{M,j}, b_j)$  is a truncated bivariate normal distribution, hence the name of bivariate-normal. The CDF of this distribution can be precisely evaluated using numerical techniques. However, since the bivariate-normal method conditions on more information than our approach does, we expect it to produce wider confidence intervals.
- MLE (approx): using the method in Panigrahi and Taylor (2022) to compute the approximate selective MLE and the corresponding Fisher information. We use the implementation available in the GitHub repository<sup>1</sup>.
- MLE (SOV): employing the SOV-based gradient descent algorithm to find the selective MLE and the corresponding Fisher information, as introduced in Section 4. In each iteration, the gradient is computed using 256 RQMC samples. These RQMC samples are generated from the Sobol' sequence, which is randomized using linear matrix scrambling followed by a digital random shift (Matoušek, 1998), using the SciPy package in Python. The step size is set to 0.01 and the algorithm stops when either the change in the log-likelihood or the change in the variable is small enough.
- CDF (SOV): CDF-based inference using SOV method. A total of 256 RQMC samples are used to construct all the confidence intervals, following the procedure derived in Section 3.2 and summarized in Algorithm 1.

For all these methods,  $\sigma^2$  is estimated by

$$\hat{\sigma}^2 = \frac{1}{n-p} \|Y - X(X^\top X)^{-1} X^\top Y\|_2^2.$$

The simulation is repeated 200 times and the results are presented in Figures 1 and 2. In Figure 1, the covariance  $\Sigma_X$  is the auto-regressive (AR) matrix with  $(i, j)$  entry being  $0.9^{|i-j|}$ , while in Figure 2 it is the equi-correlation (Equi) matrix with  $(i, j)$  entry being  $0.9 + 0.1\mathbf{1}_{\{i=j\}}$ . In both Figures, the top panels choose  $\lambda = \lambda_{\text{theory}}$  while the bottom panels choose  $\lambda = \lambda_{\text{CV}}$ . The  $x$ -axes represent the signal strength  $c_0$ . The error bars are the 95% confidence intervals produced by bootstrapping from the 200 repetitions. A few observations are in order:

- (1) The coverage probabilities of MLE (approx) method tend to fall short of the desired 0.95 coverage, especially when  $\lambda$  is selected by cross-validation. This discrepancy can be attributed to the fact that the MLE (approx) method only provides an approximate estimation of the selective MLE. In situations where the approximation is not accurate, the reliability of the method diminishes. On the contrary, the proposed MLE (SOV) method consistently achieves or even surpasses the targeted coverage probability.
- (2) The CDF-based methods, namely Splitting, Bivariate-normal, and CDF (SOV), attain the desired coverage probabilities across all scenarios.

---

<sup>1</sup><https://github.com/jonathan-taylor/selective-inference>

- (3) In terms of interval lengths, we observe a consistent order among the methods: Splitting > Bivariate-normal > SOV+IS > MLE (approx) > MLE (SOV) across all scenarios. Splitting uses the least amount of information for inference, consequently producing the longest intervals. The Bivariate-normal method, which also conditions on more information than the remaining methods, yields longer intervals than others, especially in the strong correlation scenario as shown in Figure 2. This is because when stronger correlations exist among variables, conditioning on  $\mathbf{b}_{-j}$  leaves less information in  $b_j$ , resulting in longer intervals. The MLE-based methods do not condition on the nuisance parameters as the CDF-based methods do, thus the two MLE-based methods are the shortest as expected. Interestingly, the MLE (SOV) intervals are slightly shorter than the MLE (approx) intervals, despite MLE (SOV) having higher coverage probabilities.

The wall clock times of these methods are presented in the Appendix B. While the sampling-based method entails a slightly higher computational cost compared to the approximate MLE method, which only solves a convex problem, the average inference time for each experiment is less than one second. This indicates that our method offers more reliable and accurate inference with only a minimal increase in computation cost.

## 5.2 Compare hit-and-run and SOV

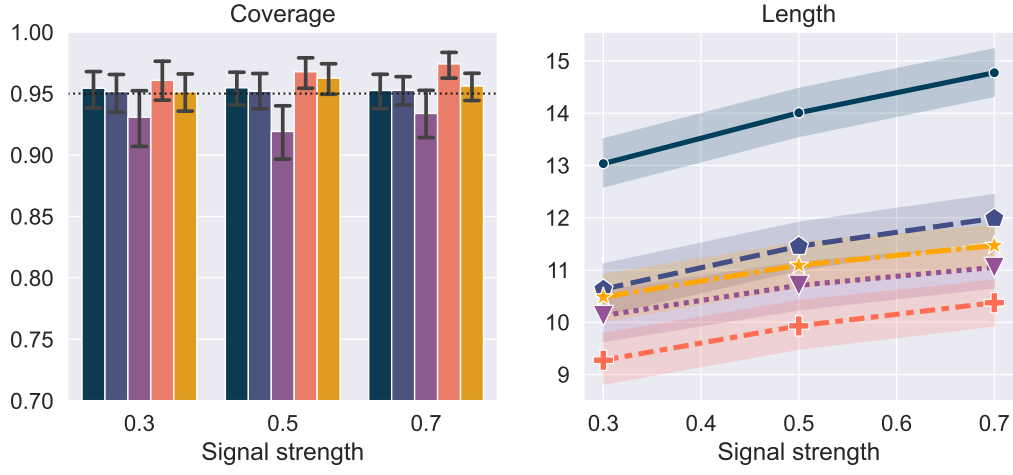
To demonstrate the superiority of the proposed SOV method to the previously used hit-and-run algorithm (Bélisle et al., 1993), we will compare their coverage probabilities, interval lengths, as well as wall clock times. The setting is the same as that in the bottom panel of Figure 1, where  $\lambda$  is selected by cross-validation and  $\Sigma_X$  is the auto-regressive matrix. The signal strength is fixed to  $c_0 = 0.7$ . The  $x$ -axis represents the number of samples  $N$  used by the two sampling methods. Note that the hit-and-run sampler uses an extra 20 samples as burn-in.

The hit-and-run sampler is used to sample  $\mathbf{b}$  from  $\mathcal{N}(\boldsymbol{\mu}_{\mathbf{b}}(\boldsymbol{\eta}), \Sigma_{\mathbf{b}}(\boldsymbol{\eta})) |_{\mathcal{O}}$  given in Corollary 2.2, with  $\theta$  set to be  $\hat{\theta}^{(2)}$ . Here,  $\hat{\theta}^{(2)}$  is the unbiased MLE of  $\theta$  obtained using the hold-out 20% data. We apply importance weighting to evaluate the CDF at different values of  $\theta$  and to compute the confidence intervals. The hit-and-run sampler is initialized at the mode of the target truncated Gaussian distribution. Finding the mode is a straightforward convex problem. The sampler moves not only in the coordinate direction, but also in the leading principal component (PC) direction of the covariance matrix of the Gaussian distribution. We use the first  $k$  PCs such that these components explain over half of the variance. Moving along the PCs allow the sampler to explore the entire distribution more efficiently, especially when there exist strong correlations. The computational overhead of finding the mode and the PCs are not factored into the computation time of hit-and-run.

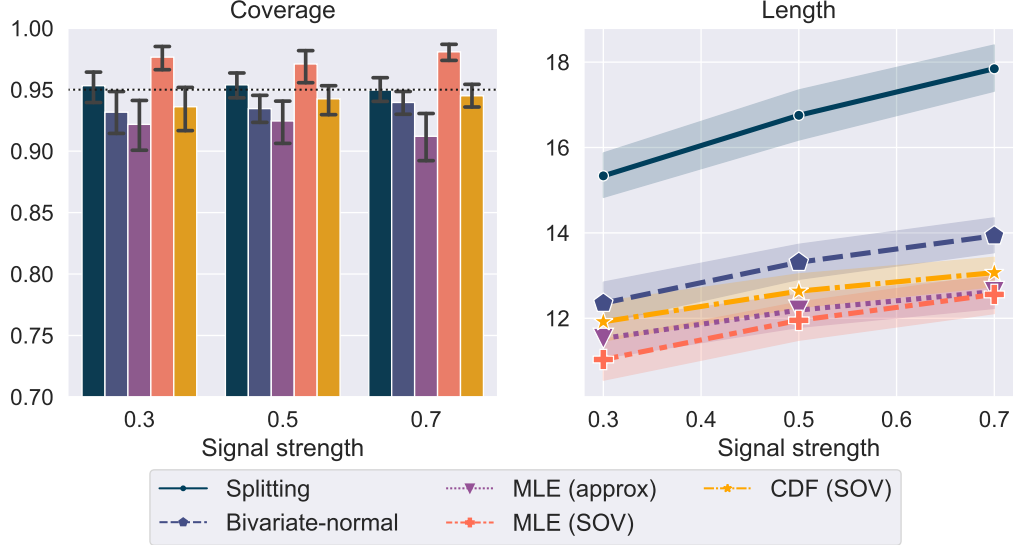
The results are shown in Figure 3. A few observations are in order:

- (1) When the sample size  $N$  is small, the hit-and-run method suffers from under-coverage, while the SOV method achieves the desired coverage even with 256 samples. As  $N$  increase, the hit-and-run method eventually achieves the same coverage as the SOV method.
- (2) For small  $N$ , the intervals generated by the hit-and-run method exhibit not only lower coverage probabilities but also longer lengths. This phenomenon could potentially be attributed to the fact that the hit-and-run algorithm is initialized at the mode of  $\mathcal{N}(\boldsymbol{\mu}_{\mathbf{b}}(\boldsymbol{\eta}), \Sigma_{\mathbf{b}}(\boldsymbol{\eta})) |_{\mathcal{O}}$ , and  $\Phi\left(\frac{\hat{\theta} - \mu_{\hat{\theta}}(\mathbf{b})}{\sigma_{\hat{\theta}}}\right)$  tends to be larger when  $\mathbf{b}$  is at the mode than on average. Consequently, when the



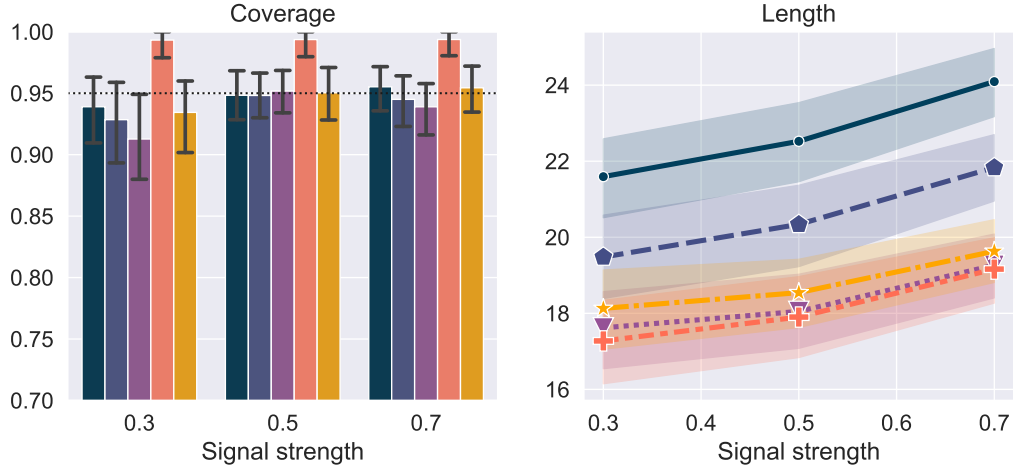


(a) Choosing  $\lambda = \lambda_{\text{theory}}$

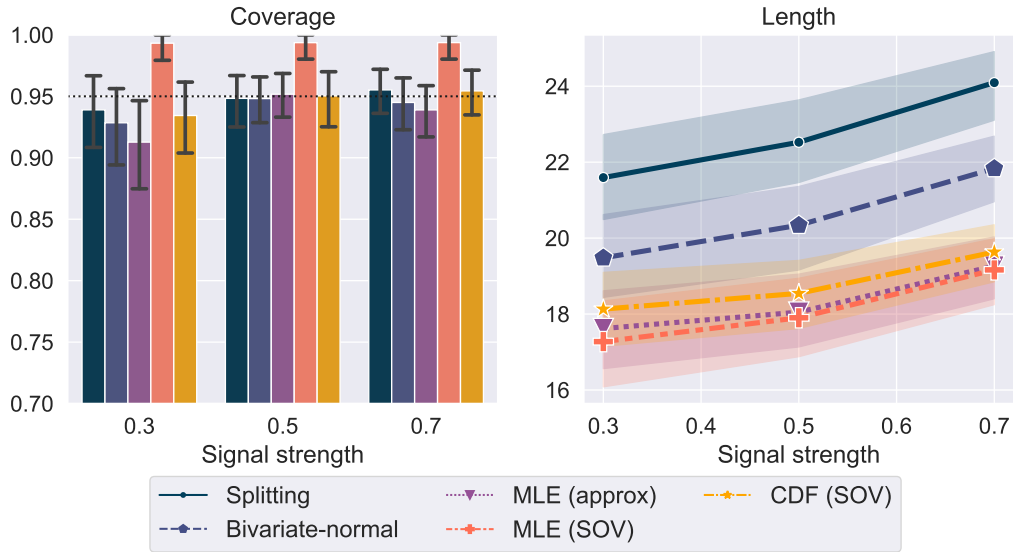


(b) Choosing  $\lambda = \lambda_{\text{CV}}$ .

Figure 1: Average coverage probabilities (left panel) and interval lengths (right panel) of intervals constructed by various methods. The targeted coverage probability is 0.95, depicted by the dotted line. The  $x$ -axes represent the signal strength  $c_0$ . In the left panel, the 5 methods from left to right are Splitting, Bivariate-normal, MLE (approx), MLE (SOV), and CDF (SOV). The error bars represent 95% confidence intervals produced by bootstrapping from the 200 repeated simulations. The regularization parameter  $\lambda$  is selected based on the theory (top panel) or through cross-validation (bottom panel). The covariance matrix  $\Sigma_X$  of the features  $\mathbf{x}_i$  is the auto-regressive matrix with  $(i, j)$  entry being  $0.9^{|i-j|}$ .



(a) Choosing  $\lambda = \lambda_{\text{theory}}$ .



(b) Choosing  $\lambda = \lambda_{\text{cv}}$ .

Figure 2: The protocol is the same as Figure 1, except that  $\Sigma_X$  is the equi-correlation matrix with  $(i, j)$  entry being  $0.9 + 0.1\mathbf{1}_{\{i=j\}}$ .

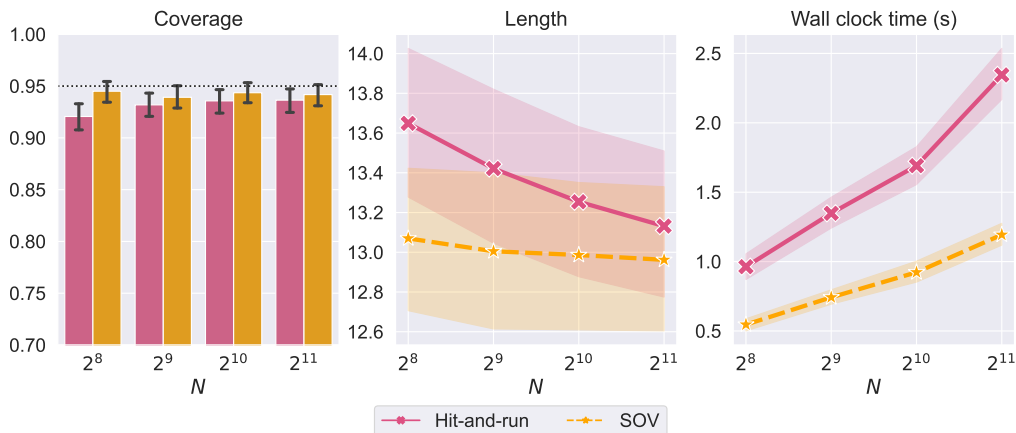


Figure 3: Compare the proposed SOV method with hit-and-run in terms of coverage probabilities (left panel), interval lengths (middle panel), and wall clock time (right panel). The experimental setting is the same as the bottom panel of Figure 1.

samples are concentrated around the mode, the resulting p-values tend to be biased upwards, subsequently leading to longer confidence intervals. As  $N$  increases, the hit-and-run sampler explores the entire distribution more sufficiently and the bias diminishes, yielding more accurate confidence intervals.

- (3) The right panel shows that the SOV method is much faster compared to hit-and-run when comparing wall clock times. This highlights the greater efficiency of the SOV method in comparison to hit-and-run.

### 5.3 Real data analysis

We consider the HIV drug resistance data from [Rhee et al. \(2003\)](#), which explores the predictive potential of various mutations for drug resistance in HIV. The response is the log susceptibility to the drug and the predictors consist of the mutations. Following [Panigrahi et al. \(2021\)](#), we focus on the drug 3TC and discard the mutations occurring fewer than 10 times in the data. This leads to a dataset of size  $n = 633$  and  $p = 91$ . We apply the lasso on a random subset of 80% of the data, resulting in 17 selected mutations.

The next goal is to compute p-values for testing whether each of selected parameter is null. These p-values are computed using the method outlined in Section 2.3. Our primary focus is to compare the proposed SOV method versus the hit-and-run method. The SOV method uses  $2^{12}$  RQMC samples, while the hit-and-run method generates  $5 \times 2^{12}$  samples, with an additional 20 samples designated for burn-in. Since both Monte Carlo estimators are random, we repeat the computation 50 times with independent randomization and use the sample standard error as an estimate of the error of the estimator.

Table 1 presents the computed p-values, accompanied by their respective error estimates enclosed in parentheses. Four variables are ignored because their p-values are extremely close to zero (smaller than  $10^{-6}$ ) indicated by both methods. The p-values obtained by the two methods are close to each

Mutations	Hit-and-run	SOV
P41L	0.98 (0.0149)	0.99 (0.0003)
P62V	0.26 (0.0165)	0.26 (0.0007)
P75I	0.70 (0.0261)	0.69 (0.0004)
P75T	0.66 (0.0136)	0.66 (0.0002)
P77L	0.47 (0.0275)	0.47 (0.0002)
P83K	0.02 (0.0046)	0.02 (0.0001)
P115F	0.12 (0.0134)	0.12 (0.0001)
P118I	0.36 (0.0111)	0.36 (0.0001)
P151M	0.12 (0.0182)	0.12 (0.0002)
P219R	0.06 (0.0058)	0.06 (0.0001)
P210W	0.24 (0.0110)	0.24 (0.0001)
P215Y	0.006346 (0.00167)	0.006428 (0.00003)
P181C	0.000073 (0.00009)	0.000097 (0.00002)

Table 1: P-values for the selected variables in the HIV data. Errors are shown in parentheses and were estimated as the standard error among 50 random replicates.

other. However, the errors of the SOV estimator are several orders of magnitude smaller than those of the hit-and-run method, even though the latter employs 5 times more samples. This highlights the remarkable precision achieved by the SOV method in contrast to the hit-and-run method.

## 6 Conclusion

Conducting conditional selective inference is often challenging due to the complexity of the conditional distributions involved. This paper developed an efficient method for sampling from such distributions, in scenarios where the selection event can be characterized by a polyhedron. Moreover, the method can be employed to compute the maximum of the selection-adjusted likelihood, facilitating efficient MLE-based inference. Empirical evaluations were performed, comparing the method against various recently proposed approaches, in the context of the randomized lasso problem.

Although primarily illustrated within the lasso framework, the methodology can be applied to other scenarios involving polyhedral selection as highlighted in the introduction. In cases with unknown covariance, the conditional distribution may involve the orthant probability of a multivariate  $t$ -distribution, for which a similar SOV method can be employed ([Genz and Bretz, 1999](#)).

## A Proofs

### A.1 Proof of Proposition 2.1

*Proof.* The joint unconditional density of  $(\hat{\theta}, \boldsymbol{\omega})$  is the product of Gaussian

$$p(\hat{\theta}, \boldsymbol{\omega}) = \varphi(\hat{\theta}; \theta, \nu) \cdot \varphi(\boldsymbol{\omega}; 0, \Omega).$$

Applying the change-of-variable formula from  $(\hat{\theta}, \boldsymbol{\omega})$  to  $(\hat{\theta}, \mathbf{b}, \mathbf{s}_{-M})$  while conditioning on  $\{\mathcal{E}, \boldsymbol{\beta}^\perp\}$ , we get the joint density

$$\begin{aligned} p(\hat{\theta}, \mathbf{b} \mid \mathcal{E}, \boldsymbol{\beta}^\perp) &\propto \exp \left[ -\frac{1}{2\nu}(\hat{\theta} - \theta)^2 - \frac{1}{2}(\tilde{Q}_1 \hat{\theta} + Q_2 \mathbf{b} + \mathbf{t})^\top \Omega^{-1} (\tilde{Q}_1 \hat{\theta} + Q_2 \mathbf{b} + \mathbf{t}) \right] \\ &\propto \exp \left[ -\frac{1}{2}(\nu^{-1} + \tilde{Q}_1^\top \Omega^{-1} \tilde{Q}_1) \hat{\theta}^2 - \frac{1}{2} \mathbf{b}^\top Q_2^\top \Omega^{-1} Q_2 \mathbf{b} + \hat{\theta}(\nu^{-1} \theta - \tilde{Q}_1^\top \Omega^{-1} \mathbf{t}) - \mathbf{b}^\top Q_2^\top \Omega^{-1} \mathbf{t} - \hat{\theta} \tilde{Q}_1^\top \Omega^{-1} Q_2 \mathbf{b} \right]. \end{aligned}$$

Let

$$\begin{aligned} \sigma_{\hat{\theta}}^2 &= \frac{1}{\nu^{-1} + \tilde{Q}_1^\top \Omega^{-1} \tilde{Q}_1}, \\ \mu_{\hat{\theta}} &= \sigma_{\hat{\theta}}^2 (\nu^{-1} \theta - \tilde{Q}_1^\top \Omega^{-1} \mathbf{t} - \tilde{Q}_1^\top \Omega^{-1} Q_2 \mathbf{b}). \end{aligned}$$

Then the above density is proportional to

$$\varphi(\hat{\theta}; \mu_{\hat{\theta}}, \sigma_{\hat{\theta}}^2) \cdot \exp \left[ -\frac{1}{2} \mathbf{b}^\top (Q_2^\top \Omega^{-1} Q_2 - \sigma_{\hat{\theta}}^2 Q_2^\top \Omega^{-1} \tilde{Q}_1 \tilde{Q}_1^\top \Omega^{-1} Q_2) \mathbf{b} + \mathbf{b}^\top (-Q_2^\top \Omega^{-1} \mathbf{t} - \sigma_{\hat{\theta}}^2 Q_2^\top \Omega^{-1} \tilde{Q}_1 (\nu^{-1} \theta - \tilde{Q}_1^\top \Omega^{-1} \mathbf{t})) \right]$$

Denote

$$\begin{aligned} \Sigma_{\mathbf{b}} &= (Q_2^\top \Omega^{-1} Q_2 - \sigma_{\hat{\theta}}^2 Q_2^\top \Omega^{-1} \tilde{Q}_1 \tilde{Q}_1^\top \Omega^{-1} Q_2)^{-1}, \\ \boldsymbol{\mu}_{\mathbf{b}} &= \Sigma_{\mathbf{b}} (-Q_2^\top \Omega^{-1} \mathbf{t} - \sigma_{\hat{\theta}}^2 Q_2^\top \Omega^{-1} \tilde{Q}_1 (\nu^{-1} \theta - \tilde{Q}_1^\top \Omega^{-1} \mathbf{t})). \end{aligned}$$

Therefore, the conditional density of  $(\hat{\theta}, \mathbf{b}) \mid \{\mathcal{E}, \boldsymbol{\beta}^\perp\}$  is proportional to

$$p(\hat{\theta}, \mathbf{b} \mid \mathcal{C}) \propto \varphi(\hat{\theta}; \mu_{\hat{\theta}}, \sigma_{\hat{\theta}}^2) \cdot \varphi(\mathbf{b}; \boldsymbol{\mu}_{\mathbf{b}}, \Sigma_{\mathbf{b}}) \cdot \mathbf{1}\{\mathbf{b} \in \mathcal{O}\}.$$

Note that  $\tilde{Q}_1 = -Q_2 \tilde{\mathbf{c}}$ . So  $\tilde{Q}_1^\top \Omega^{-1} \tilde{Q}_1 = \tilde{\mathbf{c}}^\top H \tilde{\mathbf{c}}$ ,  $\tilde{Q}_1^\top \Omega^{-1} = -\tilde{\mathbf{c}}^\top Q_2^\top \Omega^{-1}$ ,  $\tilde{Q}_1^\top \Omega^{-1} Q_2 = -\tilde{\mathbf{c}}^\top H$ . By the Sherman-Morrison formula,  $\Sigma_{\mathbf{b}}$  can be simplified as

$$\begin{aligned} \Sigma_{\mathbf{b}} &= (H - \sigma_{\hat{\theta}}^2 H \tilde{\mathbf{c}} \tilde{\mathbf{c}}^\top H)^{-1} = H^{-1} + \frac{\sigma_{\hat{\theta}}^2}{1 - \sigma_{\hat{\theta}}^2 \tilde{\mathbf{c}}^\top H \tilde{\mathbf{c}}} \tilde{\mathbf{c}} \tilde{\mathbf{c}}^\top \\ &= H^{-1} + \frac{1}{\sigma_{\hat{\theta}}^{-2} - \tilde{\mathbf{c}}^\top H \tilde{\mathbf{c}}} \tilde{\mathbf{c}} \tilde{\mathbf{c}}^\top \\ &= H^{-1} + \nu \tilde{\mathbf{c}} \tilde{\mathbf{c}}^\top. \end{aligned}$$

Moreover,

$$\begin{aligned} \Sigma_{\mathbf{b}}^{-1} \boldsymbol{\mu}_{\mathbf{b}} &= -Q_2^\top \Omega^{-1} \mathbf{t} - \sigma_{\hat{\theta}}^2 Q_2^\top \Omega^{-1} \tilde{Q}_1 (\nu^{-1} \theta - \tilde{Q}_1^\top \Omega^{-1} \mathbf{t}) \\ &= -\mathbf{k} + \sigma_{\hat{\theta}}^2 H \tilde{\mathbf{c}} (\nu^{-1} + \tilde{\mathbf{c}}^\top Q_2^\top \Omega^{-1} \mathbf{t}) \\ &= -\mathbf{k} + \sigma_{\hat{\theta}}^2 H \tilde{\mathbf{c}} (\nu^{-1} + \tilde{\mathbf{c}}^\top \mathbf{k}). \end{aligned}$$

□

## A.2 Proof of Proposition 2.3

*Proof.* It suffices to show that the denominator in (6) is proportional to (up to constants that do not depend on  $\beta_M$ )

$$\int_{\mathbf{b} \in \mathcal{O}} \varphi(\mathbf{b}; \mu_{\mathbf{b}}, \Sigma_{\mathbf{b}}) d\mathbf{b}.$$

To show this, note that

$$\begin{aligned} & \varphi(\hat{\beta}_M; \beta_M, \Sigma) \cdot \varphi(Q_1 \hat{\beta}_M + Q_2 \mathbf{b} + \mathbf{r} + \mathbf{s}; \mathbf{0}, \Omega) \\ & \propto \exp \left[ -\frac{1}{2} (\hat{\beta}_M - \beta_M)^\top \Sigma^{-1} (\hat{\beta}_M - \beta_M) - \frac{1}{2} (Q_1 \hat{\beta}_M + Q_2 \mathbf{b} + \mathbf{r} + \mathbf{s})^\top \Omega^{-1} (Q_1 \hat{\beta}_M + Q_2 \mathbf{b} + \mathbf{r} + \mathbf{s}) \right] \\ & = \exp \left\{ -\frac{1}{2} \hat{\beta}_M^\top (\Sigma^{-1} + Q_1^\top \Omega^{-1} Q_1) \hat{\beta}_M + \hat{\beta}_M^\top (\Sigma^{-1} \beta_M - Q_1^\top \Omega^{-1} (Q_2 \mathbf{b} + \mathbf{r} + \mathbf{s})) \right. \\ & \quad \left. - \frac{1}{2} \mathbf{b}^\top Q_2^\top \Omega^{-1} Q_2 \mathbf{b} - \mathbf{b}^\top Q_2^\top \Omega^{-1} (\mathbf{r} + \mathbf{s}) - \frac{1}{2} \beta_M^\top \Sigma^{-1} \beta_M \right\}. \end{aligned}$$

Let

$$\begin{aligned} \Lambda &= (\Sigma^{-1} + Q_1^\top \Omega^{-1} Q_1)^{-1} = (\Sigma^{-1} + DHD)^{-1}, \\ \mathbf{m} &= \Lambda (\Sigma^{-1} \beta_M - Q_1^\top \Omega^{-1} (Q_2 \mathbf{b} + \mathbf{r} + \mathbf{s})). \end{aligned}$$

Then the above display is proportional to

$$\begin{aligned} & \varphi(\hat{\beta}_M; \mathbf{m}, \Lambda) \cdot \exp \left[ \frac{1}{2} (\Sigma^{-1} \beta_M - Q_1^\top \Omega^{-1} (Q_2 \mathbf{b} + \mathbf{r} + \mathbf{s}))^\top \Lambda (\Sigma^{-1} \beta_M - Q_1^\top \Omega^{-1} (Q_2 \mathbf{b} + \mathbf{r} + \mathbf{s})) \right. \\ & \quad \left. - \frac{1}{2} \mathbf{b}^\top Q_2^\top \Omega^{-1} Q_2 \mathbf{b} - \mathbf{b}^\top Q_2^\top \Omega^{-1} (\mathbf{r} + \mathbf{s}) - \frac{1}{2} \beta_M^\top \Sigma^{-1} \beta_M \right]. \end{aligned}$$

Because only the first term  $\varphi(\hat{\beta}_M; \mathbf{m}, \Lambda)$  depends on  $\hat{\beta}_M$  and it is a density, so it vanishes when we integrate  $\hat{\beta}_M$  over  $\mathbb{R}^d$ . The remaining term becomes

$$\begin{aligned} & \exp \left[ -\frac{1}{2} \mathbf{b}^\top (Q_2^\top \Omega^{-1} Q_2 - Q_2^\top \Omega^{-1} Q_1 \Lambda Q_1^\top \Omega^{-1} Q_2) \mathbf{b} \right. \\ & \quad + \mathbf{b}^\top (-Q_2^\top \Omega^{-1} Q_1 \Lambda (\Sigma^{-1} \beta_M - Q_1^\top \Omega^{-1} (\mathbf{r} + \mathbf{s})) - Q_2^\top \Omega^{-1} (\mathbf{r} + \mathbf{s})) \\ & \quad \left. + \frac{1}{2} \beta_M^\top \Sigma^{-1} \Lambda \Sigma^{-1} \beta_M - \frac{1}{2} \beta_M^\top \Sigma^{-1} \beta_M - \beta_M^\top \Sigma^{-1} \Lambda Q_1^\top \Omega^{-1} (\mathbf{r} + \mathbf{s}) \right]. \quad (15) \end{aligned}$$

Let

$$\begin{aligned} \Sigma_{\mathbf{b}} &= (Q_2^\top \Omega^{-1} Q_2 - Q_2^\top \Omega^{-1} Q_1 \Lambda Q_1^\top \Omega^{-1} Q_2)^{-1}, \\ \mu_{\mathbf{b}} &= \Sigma_{\mathbf{b}} (-Q_2^\top \Omega^{-1} Q_1 \Lambda (\Sigma^{-1} \beta_M - Q_1^\top \Omega^{-1} (\mathbf{r} + \mathbf{s})) - Q_2^\top \Omega^{-1} (\mathbf{r} + \mathbf{s})). \end{aligned}$$

Recall that  $H = Q_2^\top \Omega^{-1} Q_2$ ,  $Q_1 = -Q_2 D$ ,  $Q_1^\top \Omega^{-1} Q_1 = DHD$ . By the Woodbury matrix identity,

$$\Sigma_{\mathbf{b}} = (H - HD\Lambda DH)^{-1} = H^{-1} + D(\Lambda^{-1} - DHD)^{-1}D = H^{-1} + D\Sigma D.$$

Moreover,

$$\begin{aligned}\Sigma_{\mathbf{b}}^{-1}\boldsymbol{\mu}_{\mathbf{b}} &= HD\Lambda\Sigma^{-1}\boldsymbol{\beta}_M + (Q_2^T\Omega^{-1}Q_1\Lambda Q_1^T\Omega^{-1} - Q_2^T\Omega^{-1})(\mathbf{r} + \mathbf{s}) \\ &= HD\Lambda\Sigma^{-1}\boldsymbol{\beta}_M + (HD\Lambda D - I)Q_2^T\Omega^{-1}(\mathbf{r} + \mathbf{s}).\end{aligned}$$

Since  $\Sigma_{\mathbf{b}}^{-1}H^{-1} = I - HD\Lambda D$ ,

$$\boldsymbol{\mu}_{\mathbf{b}} = \Sigma_{\mathbf{b}}HD\Lambda\Sigma^{-1}\boldsymbol{\beta}_M - H^{-1}Q_2^T\Omega^{-1}(\mathbf{r} + \mathbf{s}).$$

Also note that

$$\Sigma_{\mathbf{b}}HD\Lambda\Sigma^{-1} = (I + D\Sigma DH)D(\Sigma^{-1} + DHD)^{-1}\Sigma^{-1} = D(I + \Sigma DHD)(I + \Sigma DHD)^{-1} = D.$$

Thus

$$\boldsymbol{\mu}_{\mathbf{b}} = D\boldsymbol{\beta}_M - H^{-1}Q_2^T\Omega^{-1}(\mathbf{r} + \mathbf{s}).$$

We also have

$$D\Sigma_{\mathbf{b}}^{-1}D = DHD - DHD\Lambda DHD = (\Lambda^{-1} - \Sigma^{-1}) - (\Lambda^{-1} - \Sigma^{-1})\Lambda(\Lambda^{-1} - \Sigma^{-1}) = \Sigma^{-1} - \Sigma^{-1}\Lambda\Sigma^{-1},$$

which shows that  $\Sigma^{-1} \succeq D\Sigma_{\mathbf{b}}^{-1}D$ .

The density in Equation (15) is proportional to

$$\varphi(\mathbf{b}; \boldsymbol{\mu}_{\mathbf{b}}, \Sigma_{\mathbf{b}}) \cdot \exp \left[ \frac{1}{2}\boldsymbol{\mu}_{\mathbf{b}}^T \Sigma_{\mathbf{b}}^{-1} \boldsymbol{\mu}_{\mathbf{b}} + \frac{1}{2}\boldsymbol{\beta}_M^T (\Sigma^{-1}\Lambda\Sigma^{-1} - \Sigma^{-1})\boldsymbol{\beta}_M + \boldsymbol{\beta}_M^T \Sigma^{-1}\Lambda DQ_2^T\Omega^{-1}(\mathbf{r} + \mathbf{s}) \right]. \quad (16)$$

Note that

$$\begin{aligned}\frac{1}{2}\boldsymbol{\mu}_{\mathbf{b}}\Sigma_{\mathbf{b}}^{-1}\boldsymbol{\mu}_{\mathbf{b}} &= \frac{1}{2}(D\boldsymbol{\beta}_M - H^{-1}Q_2^T\Omega^{-1}(\mathbf{r} + \mathbf{s}))^T \Sigma_{\mathbf{b}}^{-1} (D\boldsymbol{\beta}_M - H^{-1}Q_2^T\Omega^{-1}(\mathbf{r} + \mathbf{s})) \\ &= \frac{1}{2}\boldsymbol{\beta}_M^T D\Sigma_{\mathbf{b}}^{-1}D\boldsymbol{\beta}_M - \boldsymbol{\beta}_M^T D\Sigma_{\mathbf{b}}^{-1}H^{-1}Q_2^T\Omega^{-1}(\mathbf{r} + \mathbf{s}) + \text{constant} \\ &= \frac{1}{2}\boldsymbol{\beta}_M^T (\Sigma^{-1} - \Sigma^{-1}\Lambda\Sigma^{-1})\boldsymbol{\beta}_M - \boldsymbol{\beta}_M^T D\Sigma_{\mathbf{b}}^{-1}H^{-1}Q_2^T\Omega^{-1}(\mathbf{r} + \mathbf{s}) + \text{constant} \\ &= \frac{1}{2}\boldsymbol{\beta}_M^T (\Sigma^{-1} - \Sigma^{-1}\Lambda\Sigma^{-1})\boldsymbol{\beta}_M - \boldsymbol{\beta}_M^T \Sigma^{-1}\Lambda DQ_2^T\Omega^{-1}(\mathbf{r} + \mathbf{s}) + \text{constant}\end{aligned}$$

This shows that the quantity

$$\exp \left[ \frac{1}{2}\boldsymbol{\mu}_{\mathbf{b}}^T \Sigma_{\mathbf{b}}^{-1} \boldsymbol{\mu}_{\mathbf{b}} + \frac{1}{2}\boldsymbol{\beta}_M^T (\Sigma^{-1}\Lambda\Sigma^{-1} - \Sigma^{-1})\boldsymbol{\beta}_M + \boldsymbol{\beta}_M^T \Sigma^{-1}\Lambda DQ_2^T\Omega^{-1}(\mathbf{r} + \mathbf{s}) \right]$$

is constant in  $\boldsymbol{\beta}_M$ . Therefore, the quantity in Equation (16) is proportional to  $\varphi(\mathbf{b}; \boldsymbol{\mu}_{\mathbf{b}}, \Sigma_{\mathbf{b}})$ . That is, the denominator in (6) is proportional to

$$\int_{\mathbf{b} \in \mathcal{O}} \varphi(\mathbf{b}; \boldsymbol{\mu}_{\mathbf{b}}, \Sigma_{\mathbf{b}}) d\mathbf{b}.$$

In the special case when  $\Omega = \kappa^{-1} \cdot \sigma^2 X^T X$ , we have  $Q_2^T\Omega^{-1} = DX_M^T X(\kappa/\sigma^2)(X^T X)^{-1} = (\kappa/\sigma^2)DJ_M$ , in which case

$$\boldsymbol{\mu}_{\mathbf{b}} = D\boldsymbol{\beta}_M - (\kappa/\sigma^2)H^{-1}D(\mathbf{r}_M + \mathbf{s}_M).$$

□

### A.3 Proof of Lemma 1

*Proof.* The importance weight is proportional to

$$\begin{aligned} & \exp \left[ -\frac{1}{2} \mathbf{b}^\top (\Sigma_{\mathbf{b}}(\boldsymbol{\eta})^{-1} - H) \mathbf{b} + \mathbf{b}^\top (\Sigma_{\mathbf{b}}(\boldsymbol{\eta})^{-1} \boldsymbol{\mu}_{\mathbf{b}}(\boldsymbol{\eta}, \theta) - \bar{\Sigma}^{-1} \bar{\boldsymbol{\mu}}) \right] \\ & = \exp \left[ \frac{\sigma_{\hat{\theta}}^2}{2} (\mathbf{b}^\top H \tilde{\mathbf{c}})^2 + \mathbf{b}^\top (\Sigma_{\mathbf{b}}(\boldsymbol{\eta})^{-1} \boldsymbol{\mu}_{\mathbf{b}}(\boldsymbol{\eta}, \theta) - \bar{\Sigma}^{-1} \bar{\boldsymbol{\mu}}) \right]. \end{aligned}$$

Note that

$$\begin{aligned} \Sigma_{\mathbf{b}}(\boldsymbol{\eta})^{-1} \boldsymbol{\mu}_{\mathbf{b}}(\boldsymbol{\eta}, \theta) - \bar{\Sigma}^{-1} \bar{\boldsymbol{\mu}} &= -\mathbf{k} + \sigma_{\hat{\theta}}^2 H \tilde{\mathbf{c}} (\nu^{-1} \theta + \tilde{\mathbf{c}}^\top \mathbf{k}) + Q_2^\top \Omega^{-1} (\mathbf{r} + \mathbf{s} - X^\top X_M \hat{\boldsymbol{\beta}}_M) \\ &= \sigma_{\hat{\theta}}^2 H \tilde{\mathbf{c}} (\nu^{-1} \theta + \tilde{\mathbf{c}}^\top \mathbf{k}) - Q_2^\top \Omega^{-1} X^\top X_M \mathbf{c} \hat{\theta} \\ &= \sigma_{\hat{\theta}}^2 H \tilde{\mathbf{c}} (\nu^{-1} \theta + \tilde{\mathbf{c}}^\top \mathbf{k}) - H \tilde{\mathbf{c}} \hat{\theta} \\ &= \sigma_{\hat{\theta}}^2 H \tilde{\mathbf{c}} (\nu^{-1} \theta + \tilde{\mathbf{c}}^\top \mathbf{k} - \frac{\hat{\theta}}{\sigma_{\hat{\theta}}^2}) \\ &= \Delta \boldsymbol{\tau}. \end{aligned}$$

□

### A.4 Proof of Lemma 2

*Proof.* Note that

$$\begin{aligned} \nabla_{\boldsymbol{\mu}} \log h(\boldsymbol{\mu}) &= \frac{1}{h(\boldsymbol{\mu})} \nabla_{\boldsymbol{\mu}} h(\boldsymbol{\mu}) = \frac{1}{h(\boldsymbol{\mu})} \nabla_{\boldsymbol{\mu}} \int_{\mathbf{b} \in \mathcal{O}} \varphi(\mathbf{b}; \boldsymbol{\mu}, \Sigma) d\mathbf{b} \\ &= \frac{1}{h(\boldsymbol{\mu})} \int_{\mathbf{b} \in \mathcal{O}} \Sigma^{-1} (\mathbf{b} - \boldsymbol{\mu}) \varphi(\mathbf{b}; \boldsymbol{\mu}, \Sigma) d\mathbf{b} \\ &= \Sigma^{-1} \frac{\int_{\mathbf{b} \in \mathcal{O}} (\mathbf{b} - \boldsymbol{\mu}) \varphi(\mathbf{b}; \boldsymbol{\mu}, \Sigma) d\mathbf{b}}{\int_{\mathbf{b} \in \mathcal{O}} \varphi(\mathbf{b}; \boldsymbol{\mu}, \Sigma) d\mathbf{b}} \\ &= \Sigma^{-1} (\tilde{\boldsymbol{\mu}} - \boldsymbol{\mu}). \end{aligned}$$

Similarly,

$$\begin{aligned} \nabla_{\boldsymbol{\mu}}^2 \log h(\boldsymbol{\mu}) &= \frac{1}{h(\boldsymbol{\mu})} \left[ \Sigma^{-1} \int_{\mathcal{O}} (\mathbf{b} - \boldsymbol{\mu}) (\mathbf{b} - \boldsymbol{\mu})^\top \varphi(\mathbf{b}; \boldsymbol{\mu}, \Sigma) d\mathbf{b} \Sigma^{-1} - \Sigma^{-1} h(\boldsymbol{\mu}) \right] - \nabla \log h(\boldsymbol{\mu}) \nabla \log h(\boldsymbol{\mu})^\top \\ &= \Sigma^{-1} [\tilde{\Sigma} + (\tilde{\boldsymbol{\mu}} - \boldsymbol{\mu})(\tilde{\boldsymbol{\mu}} - \boldsymbol{\mu})^\top] \Sigma^{-1} - \Sigma^{-1} - \Sigma^{-1} (\tilde{\boldsymbol{\mu}} - \boldsymbol{\mu})(\tilde{\boldsymbol{\mu}} - \boldsymbol{\mu})^\top \Sigma^{-1} \\ &= -\Sigma^{-1} + \Sigma^{-1} \tilde{\Sigma} \Sigma^{-1}. \end{aligned}$$

□

## B Computation cost

Table 2 shows the computation time in seconds of various methods in various settings. The MLE (SOV) and CDF (SOV) methods are more time-consuming. However, the computation is still



$\lambda$	$\Sigma_X$	MLE (approx)	MLE (SOV)	CDF (SOV)
$\lambda_{CV}$	AR	0.0496	0.5788	0.4356
$\lambda_{CV}$	Equi	0.0582	0.1664	0.2605
$\lambda_{theory}$	AR	0.0470	0.3789	0.2248
$\lambda_{theory}$	Equi	0.0515	0.1382	0.1652

Table 2: Wall clock time in seconds of different methods for different choices of  $\lambda$  and the covariance  $\Sigma_X$ . The experiment settings are the same as in Section 5.1. All computations were conducted on a computer node equipped with 2 CPUs, each with 4GB of memory.

reasonably fast. More importantly, the MLE (SOV) and CDF (SOV) methods are more reliable compared to MLE (approx) as shown in Section 5.1.

## References

- Bachoc, F., Leeb, H., and Pötscher, B. M. (2019). Valid confidence intervals for post-model-selection predictors. *The Annals of Statistics*, 47(3):1475–1504.
- Bachoc, F., Preinerstorfer, D., and Steinberger, L. (2020). Uniformly valid confidence intervals post-model-selection. *The Annals of Statistics*, 48(1):440–463.
- Bélisle, C. J., Romeijn, H. E., and Smith, R. L. (1993). Hit-and-run algorithms for generating multivariate distributions. *Mathematics of Operations Research*, 18(2):255–266.
- Belloni, A., Chernozhukov, V., and Wang, L. (2011). Square-root lasso: pivotal recovery of sparse signals via conic programming. *Biometrika*, 98(4):791–806.
- Benjamini, Y. and Hochberg, Y. (1995). Controlling the false discovery rate: a practical and powerful approach to multiple testing. *Journal of the Royal statistical society: series B (Methodological)*, 57(1):289–300.
- Berk, R., Brown, L., Buja, A., Zhang, K., and Zhao, L. (2013). Valid post-selection inference. *The Annals of Statistics*, 41(2):802–837.
- Blackwell, D. (1947). Conditional expectation and unbiased sequential estimation. *The Annals of Mathematical Statistics*, pages 105–110.
- Bogdan, M., Van Den Berg, E., Sabatti, C., Su, W., and Candès, E. J. (2015). SLOPE—adaptive variable selection via convex optimization. *The annals of applied statistics*, 9(3):1103.
- Casella, G. and Robert, C. P. (1996). Rao-Blackwellisation of sampling schemes. *Biometrika*, 83(1):81–94.
- Fithian, W., Sun, D., and Taylor, J. (2014). Optimal inference after model selection. *arXiv preprint arXiv:1410.2597*.
- Genz, A. (1992). Numerical computation of multivariate normal probabilities. *Journal of computational and graphical statistics*, 1(2):141–149.

- Genz, A. and Bretz, F. (1999). Numerical computation of multivariate t-probabilities with application to power calculation of multiple contrasts. *Journal of Statistical Computation and Simulation*, 63(4):103–117.
- Gibson, G. J., Glasbey, C., and Elston, D. (1994). Monte Carlo evaluation of multivariate normal integrals and sensitivity to variate ordering. *Advances in Numerical Methods and Applications*, pages 120–126.
- Hong, H. S. and Hickernell, F. J. (2003). Algorithm 823: Implementing scrambled digital sequences. *ACM Transactions on Mathematical Software (TOMS)*, 29(2):95–109.
- Kivaranovic, D. and Leeb, H. (2021). On the length of post-model-selection confidence intervals conditional on polyhedral constraints. *Journal of the American Statistical Association*, 116(534):845–857.
- Kuchibhotla, A. K., Brown, L. D., Buja, A., Cai, J., George, E. I., and Zhao, L. H. (2020). Valid post-selection inference in model-free linear regression. *The Annals of Statistics*, 48(5):2953–2981.
- Lee, J. D., Sun, D. L., Sun, Y., and Taylor, J. E. (2016). Exact post-selection inference, with application to the lasso. *The Annals of Statistics*, pages 907–927.
- Leiner, J., Duan, B., Wasserman, L., and Ramdas, A. (2021). Data fission: splitting a single data point. *arXiv preprint arXiv:2112.11079*.
- Liu, S., Markovic, J., and Taylor, J. (2022). Black-box selective inference via bootstrapping. *arXiv preprint arXiv:2203.14504*.
- Liu, S. and Panigrahi, S. (2023). Selective inference with distributed data. *arXiv preprint arXiv:2301.06162*.
- L’Ecuyer, P. and Lemieux, C. (2002). Recent advances in randomized quasi-Monte Carlo methods. *Modeling uncertainty: An examination of stochastic theory, methods, and applications*, pages 419–474.
- Markovic, J. and Taylor, J. (2016). Bootstrap inference after using multiple queries for model selection. Technical report.
- Matoušek, J. (1998). On the L2-discrepancy for anchored boxes. *Journal of Complexity*, 14(4):527–556.
- Negahban, S. N., Ravikumar, P., Wainwright, M. J., and Yu, B. (2012). A unified framework for high-dimensional analysis of M-estimators with decomposable regularizers. *Statistical Science*, 27(4):538–557.
- Niederreiter, H. (1992). *Random number generation and quasi-Monte Carlo methods*. SIAM.
- Owen, A. B. (1995). Randomly permuted  $(t, m, s)$ -nets and  $(t, s)$ -sequences. In *Monte Carlo and Quasi-Monte Carlo Methods in Scientific Computing*, pages 299–317, New York. Springer-Verlag.
- Owen, A. B. (1997a). Monte Carlo variance of scrambled net quadrature. *SIAM Journal of Numerical Analysis*, 34(5):1884–1910.

- Owen, A. B. (1997b). Scrambled net variance for integrals of smooth functions. *The Annals of Statistics*, 25(4):1541–1562.
- Panigrahi, S., Fry, K., and Taylor, J. (2022). Exact selective inference with randomization. *arXiv preprint arXiv:2212.12940*.
- Panigrahi, S. and Taylor, J. (2022). Approximate selective inference via maximum likelihood. *Journal of the American Statistical Association*, pages 1–11.
- Panigrahi, S., Taylor, J., and Weinstein, A. (2021). Integrative methods for post-selection inference under convex constraints. *The Annals of Statistics*, 49(5):2803–2824.
- Patefield, M. (2000). Fast and accurate calculation of Owen’s T function. *Journal of Statistical Software*, 5:1–25.
- Rasines, D. G. and Young, G. A. (2021). Splitting strategies for post-selection inference. *arXiv preprint arXiv:2102.02159*.
- Reid, S., Taylor, J., and Tibshirani, R. (2017). Post-selection point and interval estimation of signal sizes in gaussian samples. *Canadian Journal of Statistics*, 45(2):128–148.
- Rhee, S.-Y., Gonzales, M. J., Kantor, R., Betts, B. J., Ravela, J., and Shafer, R. W. (2003). Human immunodeficiency virus reverse transcriptase and protease sequence database. *Nucleic acids research*, 31(1):298–303.
- Schultheiss, C., Renaux, C., and Bühlmann, P. (2021). Multicarving for high-dimensional post-selection inference. *Electronic Journal of Statistics*, 15:1695–1742.
- Sobol’, I. M. (1967). Distribution of points in a cube and the approximate evaluation of integrals (in Russian). *Zhurnal Vychislitel’noi Matematiki i Matematicheskoi Fiziki*, 7:784–802.
- Tian, X., Bi, N., and Taylor, J. (2016). Magic: a general, powerful and tractable method for selective inference. *arXiv preprint arXiv:1607.02630*.
- Tian, X., Loftus, J. R., and Taylor, J. E. (2018). Selective inference with unknown variance via the square-root lasso. *Biometrika*, 105(4):755–768.
- Tibshirani, R. (1996). Regression shrinkage and selection via the Lasso. *Journal of the Royal Statistical Society: Series B (Methodological)*, 58(1):267–288.
- Tibshirani, R. J., Taylor, J., Lockhart, R., and Tibshirani, R. (2016). Exact post-selection inference for sequential regression procedures. *Journal of the American Statistical Association*, 111(514):600–620.
- Zou, H. and Hastie, T. (2005). Regularization and variable selection via the elastic net. *Journal of the Royal Statistical Society Series B: Statistical Methodology*, 67(2):301–320.